TOOL WEAR IN TITANIUM MACHINING

by

PAUL DUDLEY HARTUNG

S.B., Massachusetts Institute of Technology
(1980)

SUBMITTED TO THE DEPARTMENT OF
MECHANICAL ENGINEERING IN PARTIAL
FULFILLMENT OF THE
REQUIREMENTS FOR THE
DEGREE OF

MASTER OF SCIENCE IN
MECHANICAL ENGINEERING

at the

MASSACHUSETTS INSTITUTE OF TECHNOLOGY

June 1981

Signature of Author _____
Department of Mechanical Engineering
May 14, 1981

Certified by _____
Bruce M. Kramer
Thesis Supervisor

Accepted by _____
Professor Warren M. Rohsenow
Chairman, Department Committee

TOOL WEAR IN TITANIUM MACHINING

by

PAUL DUDLEY HARTUNG

Submitted to the Department of Mechanical Engineering on May 15, 1981 in partial fulfillment of the requirements for the Degree of Master of Science in Mechanical Engineering

ABSTRACT

The mechanism controlling the crater wear of hard cutting tool materials in the machining of titanium alloys has been shown to be fundamentally different than that in the machining of steel and nickel-based alloys. It is suggested that tool wear is greatly reduced when adhesion occurs between the tool and the chip, preventing relative sliding at the tool/chip interface. When chemical reaction occurs at the interface, tool wear may be limited by the diffusion flux of tool material through the reaction layer.

The existence of a stable reaction layer of TiC on diamond and WC-based tools (the two most wear-resistant tool materials) has been demonstrated, and the estimated diffusion flux correlates well with the observed wear rate.

Thesis Supervisor: Bruce M. Kramer

Title: Assistant Professor of Mechanical Engineering

ACKNOWLEDGMENTS

I would like to express my sincere appreciation and thanks to Professor Bruce M. Kramer for all the help and inspiration he has given me in the course of my research. A dedicated and enthusiastic educator, Bruce has been a pleasure to work with.

This work has benefited greatly from the insight and broad experience of Professor Nam P. Suh. His criticisms and suggestions have had a great influence on the direction of the work.

Ralph Whittemore, Michael Demaree, Frederick H. Anderson, John T. Ford, and Frederick P. Coté have provided invaluable assistance in the design, assembly and maintenance of the experimental apparatus.

The surface analyses which provided a theoretical basis for this investigation were conducted under the supervision of Elisabeth L. Shaw, Leonard I. Sudenfield and John R. Martin in the Center for Materials Science and Engineering.

Special thanks to the Boeing Commercial Airplane Company for having the confidence in this work to sponsor a basic re-examination of the titanium machining problem. It is hoped that future developments, based on our new understanding, will justify this trust.

TABLE OF CONTENTS

PAGE

LIST OF TABLES

LIST OF FIGURES

LIST OF FIGURES (continued)

I. Literature Review

Quite a bit of information is available on the machining of titanium. The first machinability reports were done under Air Force contracts, and as early as 1951 it was reported in Lockheed tests that milling was performed at cutting speeds from 20 to 720 sfpm (6.1 to 220 m/min) and feeds 0.004 to 0.016 ipt (0.10 to 0.41 mm/tooth). HSS, cast-alloy cobalt-chromium and carbide tools were tried. Final tests were performed with a 6-inch (15.2 cm) 6-tooth Carboloy tipped side mill with 2-1/2° neg. radial rake and 6° neg. axial rake. With the test piece in a bath of solid CO_2 and tri-ethyl phosphate (-200°K) and at speeds from 31 to 69 sfpm (9.45 to 21.0 m/min) at 0.005 to 0.008 ipt (0.33 mm/tooth) wear was slight but finish was coarse [1].

In 1954, MIT began working with the low speed turning of titanium and its alloys, using turning tests on steel as a basis for comparison and at the same time trying to build up a theoretical understanding of the cutting process in titanium [2]. The final report of this study came out in 1957 [3]. In this report, cutting forces were measured and the feed force component was found to cross the power force component before the point of total failure was reached. Tool life equations (based on Taylor) were compiled for two different alloys (C130-AM and A110-AT) and commercially pure Ti (75A).

Ceramic tools were found to be useless in machining titanium alloys at conventional speeds. Of the cutting fluids tested, aqueous $Ba(OH)_2$ was by far the most effective, and flood lubrication was most effective for water based fluids. Tests done varying the rake angles indicated that highly negative rake angle tools (side rake = back rake = -21°) yield low flank wear and that, with the conventional tool, side rake is more effective than back rake in reducing the wear rate. A nose radius of .032 inch (0.81 mm) was recommended for K2S grade carbide based on test results.

In 1955, Siekmann (Carboloy) performed some tests to determine what grades of carbide were appropriate for different conditions in the machining of titanium (Ti-150-A) [4]. In turning tests at a feed of 0.015 ipr (0.38 mm/rev) and depth of cut of 0.100 inch (2.54 mm), a cast iron grade (883) was superior to a steel grade at all speeds. With a lighter cut, the extremely hard finishing grades gave exceptional tool life. Premature failure of tools was attributed to chipping. Increasing feed was found to reduce tool life, and an optimum feed range was suggested to be between 0.008 and 0.013 inch (0.20 to 0.33 mm) feed per revolution. At 250 sfpm (76.2 m/min) both CO_2 and synthetic soluble oils gave an improvement over cutting dry, while at 500 sfpm (152.4 m/min) CO_2 helped the nose wear and the soluble oil decreased flank wear. In milling,

climb-milling was recommended to reduce chip welding; light feeds between 0.002 and 0.003 ipr (0.05 and 0.08 mm/rev) 0 degree axial and radial rake angles, 10 to 12 degree relief angle, 3 degree face cutting edge angle, and 45 degree peripheral cutting edge angle were recommended.

The increased use of titanium forgings in industry in the mid to late 1950's resulted in test programs to handle the new machining problems. In 1957, Loo [5] (North American Aviation) found that sulphurized oil gave the best tool life with carbide cutters. Dripping oil was sprayed on the cutter with compressed air to carry away the chips and to cool the cutter. The best cut lasted about seventy minutes, using a Firth Sterling NHA grade WC tool at a cutting speed of 175 sfpm (53.3 m/min) and a feed of 0.005 inch per tooth (0.13 mm); the face milling cut was 1/8 to 1/4 inch (3.17 to 6.35 mm) deep. The cut was 4 inches (10.2 cm) wide and the cutter was 6 inches (15.2 cm) in diameter. Climb milling was used. Rigidity was considered the most important influence on chip segmentation ("saw-tooth" chip formation).

In 1958, researchers at Glenn L. Martin Company did a study on various titanium milling operations, recommending that emphasis be put on secure clamping and bracing of the part, especially in the case of thin-walled forgings, and that helical carbide slab mills (45°) be used [6].

The first of a series of reports on high-speed milling at the University of Michigan was released in 1961 [7]. Three titanium alloys, A-110, B-120, and C-120, were machined at speeds from 600 to 1400 sfpm (183 to 427 m/min) for very short time durations (5 microseconds to several milliseconds) to determine whether it is feasible to increase rates of metal removal by milling at relatively high cutting speeds. Tests were performed on a lathe using work specimens with a machined stand-out profile mounted in the chuck and with Vascoloy grade 2A5, style SQ-163P cemented tungsten carbide inserts rigidly mounted in Kendex tool holders. Cutting time per chip had to be under one thousandth of a second to avoid total failure of the tool. Test results indicated that speed was more of a critical factor than cutting time per chip in determining surface finish and tool life. At 1500 sfpm (457 m/min) and cutting time per chip of 1335 microseconds, the surface finish was satisfactory, and the tools had not failed after 5 passes. At all higher speeds up to 12,000 sfpm (3660 m/min), the tool failed essentially immediately and surface finish was bad. A comparison was made between four ceramic inserts, five tungsten carbide inserts and one high-speed steel tool bit on a 1.600 inch (40.64 mm) specimen of A-110 titanium alloy at speeds from 1500 sfpm to 3000 sfpm (457 to 914 m/min). Of the tools tested, Carboloy 883 was slightly better than the 999

grade, but both grades were considered the most satisfactory. The temperature change of the tool holder was measured using a thermocouple, but this data isn't very useful, since it gives such a low estimate of actual cutting temperature. Vibrations were measured and were thought to be internal to the workpiece itself. The final report of the study on shock waves and vibrations in high-speed milling appeared in 1962 [8]. Results of impact tests and machining tests with a single-tooth cutter were compared with predicted vibrational frequencies based on shear modes, and good correlation was found. It was suggested that by superimposing a vibration of an amplitude sufficient to cause brittle segmentation and of a high frequency dynamically remote from the chatter frequencies of the system, a reduction in energy requirements could be achieved in machining.

The final phase of the University of Michigan study on the machining of titanium involved milling titanium alloys at feed rates in excess of 1000 ipm (25.4 m/min) and spindle speeds approaching 20,000 rpm with solid carbide end mills [9]. A small 2-hp high-speed air turbine was mounted in place of the tool holder on the cross rail of a 36-in. (91 cm) hydraulic planer and National Twist Drill No. 567 solid tungsten carbide 4-flute spiral milling cutters from 1/4 to 1/2 inches (6.35 to 12.7 mm) in diameter were mounted in the chuck of the turbine. Cutting velocities varied from

approximately 1200 sfpm to 2500 sfpm (366 to 762 m/min), depending on the cutter diameter, and table feed rates varied from 20 to 100 sfpm (6.1 to 30.5 m/min). Heavy wear was common to one side of the cutters and chip weld was common to all cuts. Surface finish was dependent on the tooth making the deepest cut, the most severe burr on the edge of the workpiece accompanying the area of greatest wear on the cutting edges.

A compendium on the machining of heat-resistant alloys sponsored by the USAF was published in 1962 and recommendations similar to those made by the industrial concerns in the late 1950's were made [10]. In skin milling a Ti-7.5% Mn sheet to a taper of from .050 to .025 inches (1.27 to 0.63 mm) in thickness with a 2-1/2 inch (6.35 cm) diameter carbide end mill, severe warpage and discoloration were eliminated by submerging the part to a depth of 1/4 inch (6.3 mm) in a 1-to-6 solution of commercial alcohol and water and using a 2 inch (5.80 cm) diameter, 6 flute HSS end mill. At a speed of 175 rpm (cutting speed of 28.0 m/min) and 5 ipm (12.7 cm/min) feed the part remained cool. Grumman Aircraft conducted an investigation in 1964 to determine milling parameters for 6Al-4V and 13 V-11 Cr-3Al titanium alloys and to observe certain aspects of milling these alloys under numerical control [11]. It was found that standard HSS milling cutters modified by increasing the relief

angles could be used successfully and that numerical control machining could be performed on 6Al-4V in one-half the time necessary for a similar chrome-moly steel component at 180,000 psi heat treat. Tungsten carbide (C-2 grade) cutters were recommended for face milling.

In 1965, Metcut's recommendations were quite conservative for various titanium machining operations [12]. Recommended speeds for milling were under 100 sfpm (30.5 m/min) for both HSS and carbide tools. At the same time, Boeing was using cutters with 12 carbide-tipped teeth and spray mists of 5% $Ba(OH)_2$ at 360 sfpm (110 m/min) and 140 ipm (3.56 m/min) with a cutter life of 300 feet (91.4 m) [13]. In 1965, the Defense Metals Information Center published Memorandum 199 which summarized the state of the art of machining titanium and its alloys [14]. General recommendations on rigidity of set-up, health and safety considerations (fire hazard, etc.) and handling of tools (mount to run true, grind properly, etc.) are given along with optimum cutting conditions for various carbide and HSS cutting tools in all the milling operations being performed on various titanium alloys at the time. The conditions, although given in detail, are conservative since, as is pointed out in the paper, no major break-throughs had been made in the machining of titanium alloys at that time. Water-base coolants were found to be most satisfactory for turning titanium, a 5 percent solution of sodium nitrite in water giving the best results.

Vaughn (Lockheed) did a thorough study of milling conditions for titanium alloys (A-110AT, B-120VCA, C-120AV and 6-6-2AVT), published in 1966, in which control of pertinent machining variables, such as cutting speed, feed rate, tool material, tool geometry, machine tool set-up, and cutting fluid was rigorously maintained [15]. With carbide tools, temperatures as high as 1800°F (1250°K) were noted at cutting speeds of 200 ft/min (61.0 m/min). Variables are as follows: A 4 flute end mill had 1.5 times the tool life of an 8 flute cutter under normal conditions because the small flute spaces in the multiflute end mills produced chip packing and seizing. Climb milling resulted in greater tool life than conventional milling because of reduced chip welding. Much better results were obtained from cutters ground under controlled conditions (tool life was improved by a factor of 3 in Vaughn's example) than from those showing slight burn marks, etc. For HSS end mill operations, M-2 or M-10 tools had the best tool life, as much as 4.7 times that of M-3 tools. The length of flutes for a given cutter also has a great influence on tool life - for a 1.0 inch (2.54 cm), a 2 in. (5.08 cm) flute length gave an improvement in tool life over a 3 in. (7.62 cm) flute length by a factor of about 3. Radial depth of cut was shown to have an influence on tool life, and at lighter depths of cut the effect of varying the speed becomes more prominent. Tool

life dropped drastically when the feed was varied from the optimum, stressing the point that the optimum feed rate for a given cutting speed/cut geometry is most important when machining titanium.

Two papers were presented in a conference on Machinability in 1965 and were published in 1967. One of the papers [16] deals with metallurgical factors affecting the machinability of titanium and the other [17] has, essentially, a practical approach to the machining of titanium. The first [16] points out that (as had been previously reported by Vaughn and others) the difficulties cannot be attributed to work hardening, but that the thin chip resulting from the high shear angle, the absence of a built-up edge to dissipate heat and the very low thermal conductivity of titanium alloys lead to much higher surface heating of the tool and contamination of the titanium. It was also suggested that the higher pressure produced by the thin chip coupled with the high heat generated lead to pressure welding of the chip to the tool.

The second paper [17] makes the statement that titanium is not difficult to machine and that rigid machine tools with adequate power, speeds and feed will solve the problems with machining titanium. Surface treatments with solid lubricants such as Sulfiniz, molybdenum disulphide, graphite, etc., have not proved any great benefit, as they appear to be removed rapidly from the tool surface and are carried away

on the first few chips. Of chemically active cutting fluids tried, phosphates gave the best results and showed great promise as a cutting medium, but suitable corrosion inhibitors were not found before improvements in tool materials made further work on these fluids "unnecessary." Chlorinated cutting fluids were found effective but were banned because of their toxicity. Chlorokerosenes were found to be equally effective without the attendant risks.

In 1968, the results of a Metcut study were published, which dealt mainly with the surface effects, such as residual stresses, produced in manufacturing operations, but which gave some recommendations for machining conditions for titanium alloys [18]. For peripheral end milling of Ti 6Al-4V, superhard high speed steel grades (M41-M45 series) indicated some advantage over tool materials such as M-2. A feed of .003 in. (.076 mm) per tooth and a cutting speed of 145 sfpm (44.2 m/min) provides about a 25% higher metal removal rate than a feed of .002 in. (.051 mm) per tooth and a cutting speed of 170 sfpm (f1.8 m/min). The effect of heavy cuts on cutter life was explored at 180 sfpm (54.9 m/min) and .003 in. (.076 mm) per tooth. Two and one half times greater tool life was obtained at a depth of cut of .125 in. (3.17 mm) and width of cut of .375 in. (9.52 mm) than with a cut where both of those dimensions were doubled.

In 1970, LeMaitre published a paper on the machining of

titanium and its alloys in which he reports on the results of micro-milling tests (along with other types) in which cutting forces were measured and cutting energies calculated [19]. Soluble oils containing MoS_2 and Sulfochlorinated soluble oil in 5% solution gave the best results. He suggests that at ultra-high speeds the effect of lubrication will be non-existent. Analytical study of chip flow is based on turning tests and he showed that the fracturing of chips is possible through modification of tools. These modifications, which consisted of channel-like grooves, aided in lubrication, giving better performance and output, particularly in drilling and tapping.

Much of the preceding literature review was made possible by the excellent list given by Kreis in the German literature in 1974 [20].

The recent interest in achieving higher metal removal rates in the machining of titanium alloys has led General Electric to conducting quite a bit of research in titanium machining. In the 1980 Annual Technical Report of G.E.'s Advanced Machining Research Program, papers were presented on chip formation [21, 22], alternative tool designs [23] and pulse laser experiments [24], as well as on high-speed machining of titanium with various tool materials, both in the lab [25] and in production [26].

Komaduri [21] has studied the mechanism of chip formation

of Ti 6Al-4V in machining studies conducted at various cutting speeds up to 800 sfpm (244 m/min) under orthogonal cutting conditions and up to 1000 sfpm (305 m/min) on a lathe [22]. An extremely low speed (12.7 micron/min [.050 in/min]) experiment was performed inside a Scanning Electron Microscope (SEM) and the cutting process was monitored with a video tape. The higher speed orthogonal cuts were monitored with a Hi-Cam, high-speed movie camera (8000 frames/sec). Photomicrographs were taken of longitudinal cross-sections of chips. All of these studies have shown that the mechanism of chip formation doesn't change much with cutting speed. The chip formation is an inhomogeneous process which occurs periodically and in two stages. The bulk of the chip segment is formed by a gradual softening of a half wedge of titanium ahead of the tool and once the chip segment has reached its final shape very intense deformation occurs in a narrow band separating the segments. There is very little further deformation of the segment after this point in the process.

Komanduri has performed experiments with Laser-Assisted Machining (LAM) and machining a preheated billet of Ti 6Al-4V and had found that it is possible to modify the usual periodic catastrophic shear-failed chip to a more continuous chip by heating the work material ahead of the shear zone to a high temperature [22]. He believes that this facilitates an alpha to beta allotropic transformation of the titanium.

Cutting forces were reduced by about 50% with LAM, and the continuous chip should reduce chatter. The material handling problem of the preheated workpiece is difficult enough to make that method unfeasible in production. The success of eht LAM approach depends largely on the ability to heat the work material right ahead of the shear zone without heating the material near the tool tip. The high temperatures near the tool tip could cause rapid plastic deformation and accelerated wear of the tool.

Lee [23] has worked on developing tools which can cut effectively at high speeds when worn. One approach he has taken has been to form a laminated tool which will behave like a thin tool whose thickness is less than the maximum allowable wear land. Experiments have been performed with ceramic tool bodies of hot pressed silicon carbide and aluminum nitride with thin plates (0.75 mm thick) of cemented carbide brazed on the top surface. These ceramic materials wear rapidly in the machining of titanium alloys, but the cemented carbide determines the geometry of the cut. Problems with delamination seemed to limit the success of these tools. The idea with the composite tools is to create a ledge by wearing the tool material under the plate which comes in contact with the workpiece and to extend tool life by controlling flank wear.

An alternative approach has been to grind a ledge on

standard grade 883 carbide cutting tools [23]. The width of the ledge for each tool is chosen to be equal to the depth of cut to be taken and the thickness of the ledge to be chosen as the ultimate flank wear size to be tolerated. The tool is positioned with the edge of the ledge almost parallel (less than 1 degree) to the finished surface of the workpiece, somewhat like a broadnosing cut. Turning tests were performed on fully heat treated Ti 6Al-4V at cutting speeds from 180 m/min (585 sfpm) to 360 m/min (1170 sfpm) at a feed rate of 0.225 mm (0.009 inch). Tools with 5° back and side rake were used. Depth of cut was varied from 0.75 mm (0.030 inch) to 1.25 mm (0.009 inch) depending on the width of the ledge used. The cutting edge wore rapidly, but moved along the length of the ledge in such a way that the tools cut efficiently even after a large portion of the ledge was worn away. Tool life at 180 m/min was about 20 minutes. Similar results were achieved in face milling a forged 6-2-4-2 titanium alloy block at a feed rate of 0.085 mm (0.0034 inch) per tooth. Ledge breakage was only a problem at speeds over 300 m/min. Surface finish was reported to be excellent in turning and milling. It is not clear why these ledged tools perform as well as they are reported to, since flank wear doesn't generally limit tool life at high cutting speeds, and since the plastic deformation of the grade 883 carbide material should be very rapid at the higher speeds tested.

More information must be obtained on these tools before any conclusions can be made.

Experiments were performed with pulsed laser to determine the effect of weakening the titanium workpiece surface by drilling a large number of holes ahead of the cut [24]. A bar of Ti 6Al-4V was predrilled and turned at 100 sfpm (30.5 m/min) with Carboloy 883 grade cemented tungsten carbide. Cutting forces were reduced by as much as 28% in a couple of cases and tool wear was reduced. The pulsed laser was attached to the carriage of the lathe and tests were performed with he laser operating while the cut was being made, like in LAM. Cutting speed was limited to 60 sfpm (18.3 m/min) in these tests because of the limits of the laser, and although tool wear seemed to be reduced slightly, cutting temperatures increased. Tests need to be performed at higher cutting speeds to see whether forces are reduced significantly enough to reduce tool wear, or whether the temperature rise and intermittent nature of the cut are detrimental to tool life.

G.E. performed conventional turning tests with various carbide grades, ceramics and Borazon^{R} at cutting speeds up to 1200 sfpm (366 m/min) comparing cutting forces, chip thicknesses and tool wear among the tool materials tested. As could be expected, ceramics and Borazon^{R} failed rapidly at all the speeds tested. The best grade of carbide tested was

Carboloy 883, but none of the grades tested have good thermal deformation resistance, so cutting speed was limited to 600 sfpm (183 m/min) with the tools failing in a matter of seconds at this speed. Cutting forces were found to be more dependent on feed than speed and didn't decrease with speed.

II. Discussion

In approaching the problem of achieving higher metal removal rates in the machining of titanium, particularly in milling, it is clear that either temperatures have to be reduced through a new method of cooling and/or a cutting material must be found which is not only hard at high temperatures but which can withstand the thermal and mechanical shocks and the chemical attack that are associated with titanium machining. All possibilities for achieving these effects must be considered.

Lubrication

It is possible that lubricants can be found which will reduce friction at the tool-chip interface, but it is not clear whether a lubricant will be effective at higher cutting speeds. An analysis of lubricant action combined with new techniques of applications may answer this question. Cook et al. [27] achieved good results with continuous electroplating at lower cutting speeds in 1966, obtaining an improvement in tool life of 2 to 8 times that of an

unlubricated tool, but the corrosive action of the fluids made the method undesirable in practice. Vaughn in recent communications stated that he thinks that there is a possibility for success in this area of research, and no one has followed up on it [28].

In 1971, Uehara et al. [29] proposed a new technique (devised in 1969 by them) in which a wide variety of metals, ceramics and oxides could be thermo-sprayed on to the rake and clearance surfaces of the cutter during non-cutting in an intermittent operation such as milling. The effect on cutting performance was found to decrease with speed, and a suitable metal was not found in preliminary tests, but there is no necessity to protect the machine against corrosion since this method uses no electrolyte. Uehara went on to try a simple method of coating solid lubricants on the surface of the workpiece by mixing the solid lubricants in a viscous medium such as grease, vaseline, etc. [30]. In the machining of steel the method was determined to be effective in decreasing cutting forces (especially the thrust force) and decreasing flank and crater wear at 100 m/min, and effective in decreasing crater wear at the speeds over 150 m/min. Cutting speeds as high as 300 m/min were tried.

In 1978, Koury et al. [31] reported on a study in which milling cutters were coated with solid film lubricants using various binders and pigments (solid particles). In Phase I,

Ti 6Al-4V was machined (along with AISI 4340 and L-605) at 24 m/min for 50 minutes. The cutter was an M-2 HSS. Best results were obtained with an MoS_2 + metallic oxide-modified epoxy resin binder coating. Cutting force, surface finish and flank wear were improved. In Phase II production testing, a 50.8 mm diameter (2 in.), 6 flute M-2 HSS cutter was run at 35.7 m/min (117 sfpm) at a feed of 2.0 m/min (78.7 ipm) and axial depth of cut of 55.8 mm (2.2 in.) to evaluate the coating metioned above in machining an engine support track with a vertical milling machine. This was a peripheral end milling application (climb mode). In production, neither surface finish nor flank wear were improved by the coating as compared to the uncoated cutter. The coating was quickly removed.

If solid lubricants are to be applied, the process will have to be a continuous one, such as Cook's [27] or Uehara's [29] metallizing approach. At higher cutting speeds on titanium, however, the effect of the coating may be reduced by the forceing of the coating from the interface.

High Speed Machining

It has been suggested on several bases that tool wear may decrease at high speeds. Ultra-high speed machining has been successfully applied to the machining of aluminum by creating a condition of "catastrophic adiabatic shear" where reduced cutting forces result in a reduced cutting temperature. Vaughn did extensive experiments using ballistics in the late 1950's

and early 1960's and found that at cutting speeds on the order of 100,000 to 120,000 sfpm (30,500 to 36,600 m/min) the cutting forces and temperature were actually reduced in titanium and steel [32]. He simulated these high speeds with a specially designed serrated cutter on a high speed low-torque planer with turbine-operated motor and on a larger scale with a cutter mounted on a rocket powered sled [28].

Recht [33] developed a model of the catastrophic shear mechanism which is believed to occur during ultra-high speed machining and ballistic impact. The mechanism seems to be similar to the stage of intense deformation in a narrow band in the formation of the segmented chip while machining titanium [22]. A reduction in cutting forces and temperatures has been predicted to occur at some critical cutting speed for all work materials. Several studies have been performed with high speed lathes on steel, brass and aluminum to determine whether this critical speed could be reached with modern machinery [34, 35, 36]. It was found that in the machining of aluminum at very high cutting speeds, there is no tool wear problem. A Metcut survey in 1978 showed that industrial concerns were machining aluminum at speeds up to 12,000 sfpm (3660 m/min) [37]. In this same survey, which was an international survey of industrial and academic research, the only high speed machining of titanium which was reported was the work done at the University of Michigan in the early 1960's [7, 8, 9].

More theoretical work on ultra-high speed machining was done in an effort to predict cutting forces from work material properties [38, 39, 40].

In 1970, Arndt predicted that practical machine tools could be designed in which ultra-high speeds are obtained by explosive, hydraulic or pneumatic means for straight-line machining, or by electro-magnetic or turbine-drive for rotary machining [41]. In 1972, he published some experimental results obtained with a new ballistic testing facility [42].

King [43] reported in 1976 on a test facility at Lockheed which contained three machines for very high speed machining research. A Sundstrand, numerically controlled, five axis, Model OM-3 mill with replacement spindles had a continuously variable speed range up to 100,000 rpm and a maximum table feed of 194 in/min (4.93 m/min). Cutter diameters up to 1 inch (2.54 cm) could be used at midrange spindle speeds and cutter diameters up to 1/4 in could be used at the higher speeds. This allows cutting speeds up to about 6,500 sfpm (1980 m/min). A Bullard 36-in (91.4 cm) vertical turret lathe was modified to include a table capable of turning 600 rpm and a milling head on the ram which is capable of turning 6000 rpm with formed cutters up to 8 inches (20.3 cm) in diameter. This allows cutting speeds up to about 12,500 sfpm (3810 m/min). A horizontal lathe test bed was being designed with a maximum speed of 10,000 rpm which could handle test

samples up to 18 inches (45.7 cm) in diameter. This would allow cutting data to be taken at speeds up to about 50,000 sfpm (15,000 m/min). At the time of the report, the only material which was being machined was aluminum. Two examples were given of production parts which were end milled at speeds over 5,000 sfpm (1,500 m/min) with reduced cutting forces, improved part stability and improved surface finish over conventionally machined parts. Less distortion was found in thin-walled parts machined at very high speeds, and plunge milling of aluminum at very high speeds seemed promising. The only limitation to additional progress was thought to be the strength of machine tool materials.

The most recent research in ultra-high speed machining is being conducted at General Electric [44, 45]. Two ballistic test facilities are being used to test a variety of work materials. Tests are planned on titanium alloys, but no results have been published yet.

Cryogenic and Hot Machining

Cryogenic cooling has been used with some success as reported with CO_2 in the 1950's on titanium [1, 4]. At Douglas Aircraft, ABC)-156 Solvolene, a coolant which maintains a temperature of 233°K was being used in production turning and milling of titanium with an improvement in surface finish [46]. In a variety of duplicating operations on a Gorton pantograph type machine, a large improvement in cutter life at high

cutting speeds was achieved with cooling in machining titanium. In the milling and duplicating operations, the part was immersed in a reservoir attached to the machine bed 15 minutes prior to and during the cut.

Leith, Carr and Heine published a report in 1960 (AMC Tech. Report 60-7-681) in which cooling was accomplished by (1) application of CO_2 mist at the cutting edge; or (2) flooding both workpiece and tool with ABC0156-A Solvolene; or (3) chilling the workpiece in a cold chest prior to machining. Increases in tool life and cutting speed were reported, but only an abstract is available for review at this time [47].

In 1965, Grumman Aircraft performed cutting tests on Ti 6Al-4V and Ti 6Al-4V-2Sn titanium alloys with direct nozzle application of both liquid nitrogen and liquid carbon dioxide [48]. In slotting tests on Ti 6Al-4V with a 5/8 inch (15.9 mm) diameter, 4 flute, standard M-2 end mill at 0.125 inch (3.18 mm) depth of cut and 0.0024 ipt (0.061 mm/tooth) chip load at 100 sfpm (30.5 m/min), a 70 percent improvement in tool life was noted with liquid CO_2 and 240 percent improvement with liquid N_2. Liquid nitrogen was also used in turning operations with a greater improvement in metal removal rate than was achieved in the slotting tests. In drilling, cryogenic cooling only seemed effective on shallow holes, such as in the drilling of sheet stock.

It is known that the Technical University of Aachen is

conducting research in the use of liquid nitrogen cooling for machining titanium. A request for further information [49] indicated that significant increases in tool life were obbained, but that the added cost of providing liquid nitrogen was greater than the savings due to increased life. Only limited information is available, since the details of the research are confidential.

At M.I.T., Joshi [50] has been experimenting with liquid nitrogen as a cryogenic coolant for profile milling titanium alloys. In tests on Ti 6Al-4V with high speed steel end mills, he has found that a combination of liquid N_2 and soluble oil reduces tool wear possibly by providing a solid lubricant action and/or improving the heat transfer rate. Since his tests were conducted with HSS, cutting speeds were limited to 52.5 sfpm (16.0 m/min) and 61.5 sfpm (18.8 m/min). At these speeds, powder metal and M42 grades of HSS gave improved tool life over M7 grade due to their higher hardness and a reduction in friction from the cobalt in their compositions.

In 1963, Dickter et al. [51] in a final report on high temperature machining methods did a series of turning and milling tests on Ti 6Al-4V at various elevated workpiece temperatures in an argon atmosphere, demonstrating a definite decrease in tool life occurring around 900°F to 1300°F (755°K to 978°K). The decrease in tool life is most likely due to rapid plastic deformation of the carbide tools at the elevated temperatures.

New Tool Materials

Although quite a bit of work has been done in the last thirty years in an effort to find the limits of application of HSS and cemented WC tools in the machining of titanium and its alloys, very little work has been done with alternative tool materials.

Much of the following discussion is based on the present work. In order to achieve higher metal removal rates in machining titanium alloys, a tool material will have to be found which will maintain its mechanical integrity at high cutting temperatures, and which will not wear rapidly at high cutting speeds. Existing ceramic tool materials have good high temperature mechanical properties but react violently with titanium upon contact with the workpiece. Polycrystalline cubic boron nitride (Borazon^{R}) has been shown to wear at a high rate at conventional cutting speeds (approx. 60 m/min) and react violently with titanium at high cutting speeds (approx. 300 m/min). Existing coated carbide tools encounter problems with coating delamination and wear at a more rapid rate than uncoated C3 grade cemented carbide. Test results in continuous turning of Ti 6Al-4V at cutting speeds from 200 sfpm (61.0 m/min) up to 400 sfpm (122 m/min) indicate that a C3 grade (WC-5.8% Co) cemented carbide is more wear resistant than all other tool materials commonly used in the machining of superalloys. At cutting speeds of 400 sfpm (122 m/min) and higher, the carbide tool fails within a couple of minutes

by plastic deformation of the cutting edge.

The only tool material which was found to be both more wear resistant and more deformation resistant than the WC tool is polycrystalline diamond. Polycrystalline diamond was tested at cutting speeds up to 1500 sfpm (457 m/min), and the material shows quite a bit of promise in the high speed machining of titanium alloys. Polycrystalline diamond tool materials are presently only being made by three companies: General Electric, DeBeers, and Megadiamond. General Electric has found its Compax^{R} tools unsuitable for ferrous and nickel-based alloys because of their affinity for carbon [52]. Compax has been reported to be most effective on hard, abrasive materials which are chemically rather inert to carbon, such as ceramic materials, carbonaceous materials copper and aluminum alloys (including silicon-aluminum), glass fiber reinforced materials, etc. [53]. General Electric has not released any reports of machining titanium alloys with Compax. The application they have most recently been interested in has been the machining of cast aluminum alloys [54, 55].

In 1977, DeBeers described machining tests on Ti 6Al-4V which compared the performance of Syndite^{R} (DeBeers polycrystalline diamond) tool made from a 90° segment brazed to a steel shank to that of multi-coated carbide tool in turning a 65 mm square x 145 mm long billet to a diameter of 64 mm [56, 57]. At a cutting speed of 56 m/min (184 sfpm) the carbide tool was badly worn after a single pass over a length

of 70 mm, representing a total stock removal of 0.07 cm^3. The Syndite tool, under the same intermittent cutting conditions, was able to remove 132 cm^3 of material before showing signs of comparable wear. Excellent surface finish was obtained with the Syndite tool, which was tested at depths of cut up to 3 mm with good results. The coated carbide tool is not a good basis for comparison (my tests show that coatings significantly increase the wear of the carbides), but the results from the Syndite tool are impressive in their own right.

DeBeers published a series of reports on Syndite^R in 1979 that reported tests of the material in various machining applications, as well as wire drawing, grinding wheel dressing and rock drilling applications. Turning tests were performed on Ti 6Al-4V and Syndite^R was shown to give twice the stock removal rate of a tungsten carbide tool in this application (under their equivalent chip thickness criterion [58]. At this ratio, the cost of using diamond tooling is prohibitive.

The idea of using diamond for machining titanium is not new in that diamond turning tools have been used to achieve high surface finishes on space vehicle components since as early as 1976. In an article by Milbrandt in Industrial Diamond Review in that year, diamond turning tools were reported to give not only better surface finish, but also to have

performed operations on thin-walled parts which were difficult to perform without distortion of the part when using carbides [57]. The diamond lathe tools showed excellent life and could be used at four times the cutting speed that carbides were being used at for the same operations.

III. Introduction

In order to develop new cutting tool materials, a comprehensive evaluation of potential tool materials was undertaken in an effort to determine which of these might be the most wear-resistant and what material properties are critical in determining the wear resistance.

Because of the relative simplicity of the geometry of the process and the continuous nature of the cut, the turning process was chosen as the appropriate test to determine the basic wear properties of the various materials.

IV. Experimental Procedure

Only a limited number of potential tool materials are available in solid form. Cemented tungsten carbide, cemented titanium carbide, complex carbides based on tungsten carbide, ceramics, cermets, polycrystalline diamond and polycrystalline boron nitride are the only materials that are presently being produced in solid form that have the thermo-mechanical properties that are necessary for high speed metal cutting. In order to determine the wear resistance of other potential tool materials in a given application, coatings of the materials of interest must be applied to one of the standard tool materials. The wear of the coating is then observed.

The first phase of the testing involved the identification of a suitable carbide to use as a basis for comparison

and as a substrate for coating. Kennametal K68 (C3 grade) cemented tungsten carbide (5.8% cobalt) and Kennametal K7H (C8 grade) complex carbide have been coated at M.I.T. with a variety of refractory carbides [60] and were therefore of interest as potential substrates. Kennametal K68 is the grade which Kennametal recommends for machining titanium alloys and superalloys. The Surftech Corporation produces coatings of hafnium carbide and zirconium carbide, so Surftech H-25x (C2 grade) and Surftech H-2S (C3 grade) cemented tungsten carbide substrate materials were evaluated in turning Ti 6Al-4V. Carboloy 820 (C2 grade) inserts, which are used in industry to machine titanium, were also tested.

To reduce plastic deformation of the cutting edge at higher cutting speeds, and to optimize the number of available cutting edges per tool, square negative rake inserts of SNG 432 geometry were chosen for the tests. The Carboloy SBTR-16-4 tool holder has back and side rake angles of -5°, and was mounted to give a side cutting edge angle of 15°. Depth of cut was chosen to be .050 in. (1.27 mm) so that wear of the tool would extend well beyond the 1/32 in. (0.79 mm) nose radius of the tools without wasting more workpiece material per test than is necessary to determine the tool wear rate. The feed rate was standardized to .005 ipr. (0.127 mm/rev.).

The cutting tests were performed on an instrumented American Pacemaker 14x30 lathe. The lathe is powered by an

18.6 kW (25 horsepower) D.C. motor, and the speed is continuously variable (Figure 1).

Force measurements were made with a strain gage type tool post, three component force dynamometer, and were recorded on a Sanborn Model 321 chart recorder. The dynamometer was replaced with a rigid tool post when tests were performed to determine tool wear, since the rigidity of the machine tool is so critical in machining titanium alloys.

Cutting temperatures were measured using the tool/chip thermocouple method, where the thermal EMF between the tool and the workpiece is measured. The average temperature over the tool/chip contact area is measured directly in this way. The tool/chip thermocouple is calibrated by taking a long chip of workpiece material and a long piece of tool material as the leads of a thermocouple and measuring the voltage between them against a known thermocouple, such as Chromel/Alumel in a molten metal bath (aluminum or tin). The errors involved in this method are mainly due to the thermal EMF effect between the tool and the tool holder, and the difficulty of maintaining cold juctions during calibration. However, this is probably the best method for measuring cutting temperatures at this time [61]. Cutting speed was measured immediately prior to the tests with a tachometer, and the lathe speed was set to the desired value. Cutting time was measured with a stop watch.

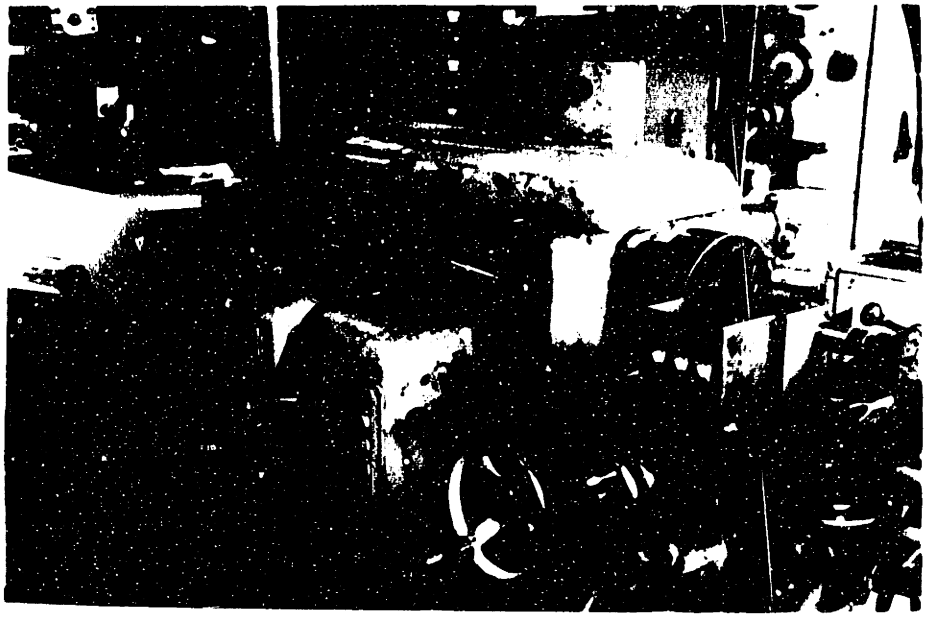

a

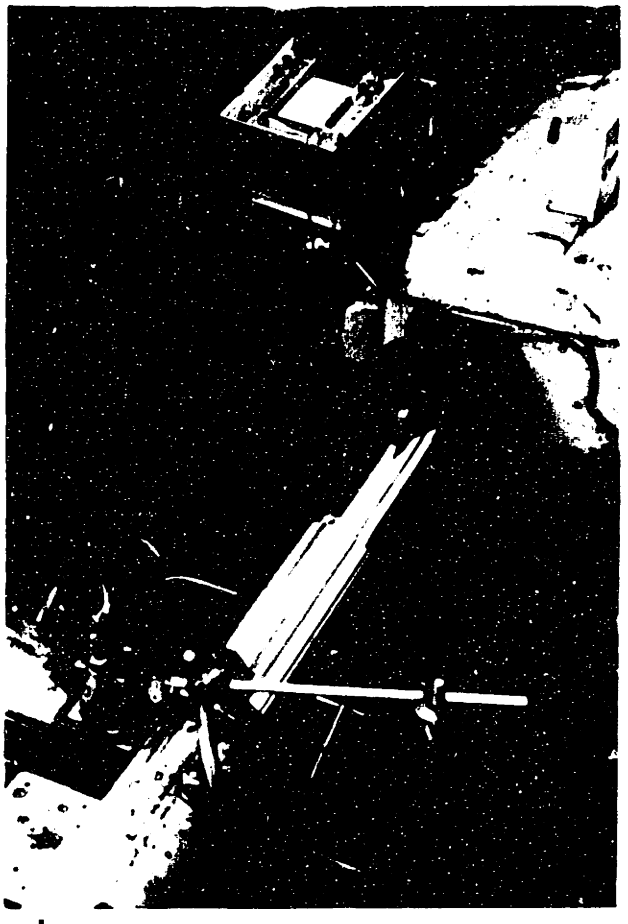

b

Figure 1. American Pacemaker Lathe Instrumented for a) Force Measurement and b) Temperature Measurement

Tool wear was observed and the flank wear measured with a toolmaker's microscope at various cutting intervals. The wear on the rake face was measured at three locations using a Taylor-Hobson Model 3 Talysurf, stylus-type, surface measuring instrument. Chips and used tools were saved for later observation.

V. Baseline Tests

Of the five potential substrate materials tested, Kennametal K68 (C3) and Carboloy 820 (C2) performed the best. At a cutting speed of 200 sfpm (61.0 m/min) the tool life of these materials is over 20 min. with no significant plastic deformation. Kennemetal K68 shows very little flank wear at this speed (.0035 in. (.089 mm) after 29 min.) and the crater wear rate is approximately 2.2 microns/min. Carboloy 820 (C2) has slightly greater flank wear (.0060 in. (.152 mm) after 20 min.) but the crater wear rate (2.0 microns/min) is about the same as that of K68. The Kennametal K7H (C8) material had a tool life of less than 10 minutes at this cutting speed, with over .020 in. of flank wear and a crater wear rate of 5 microns/min. The Surftech H-25X (C2) material was by far the worst of the potential substrate materials. The tools failed in about 5 minutes due to gross plastic deformation of the cutting edge, and the crater wear rate was approximately 8 microns/min. The measured cutting forces were also higher for the H-25X substrate than the K68 substrate. The

power force and feed force components were 1.2 and 1.8 times higher for the H-25X material. Surftech H-2S (C3) had a crater wear rate of about 4.2 microns/min, with .012 in. of flank wear after 5 min. of cutting at 200 sfpm.

Tests were performed at cutting speeds from 50 to 2000 sfpm (15.2 to 610 m/min) on Kennametal K68 (C3) and at speeds from 200 to 300 sfpm (61.0 to 91.4 m/min) on Carboloy 820 (C2). The crater wear rates of these materials increase with cutting speed (see Figure 2) and was the primary cause of tool failure at speeds up to 350 sfpm (107 m/min). At 400 sfpm (122 m/min) plastic deformation of the cutting edge caused the tools to fail after two minutes of cutting, due to the high temperatures generated at that cutting speed.

To determine the relative wear rates of the various potential tool materials in the machining of Ti 6Al-4V titanium alloy, turning tests were performed at 200 sfpm (61.0 m/min) using various coated and uncoated carbides, polycrystalline cubic boron nitride and polycrystalline diamond. Cutting tools tested and number of tests performed on each are listed in Table 1. The average crater wear rates of the various tool materials in turning Ti 6Al-4V at 200 sfpm are shown relative to each other in Figure 3.

Preliminary cutting tests were performed on C 130AM titanium alloy under the same conditions that were subsequently maintained in the machining of Ti 6Al-4V, at cutting speeds

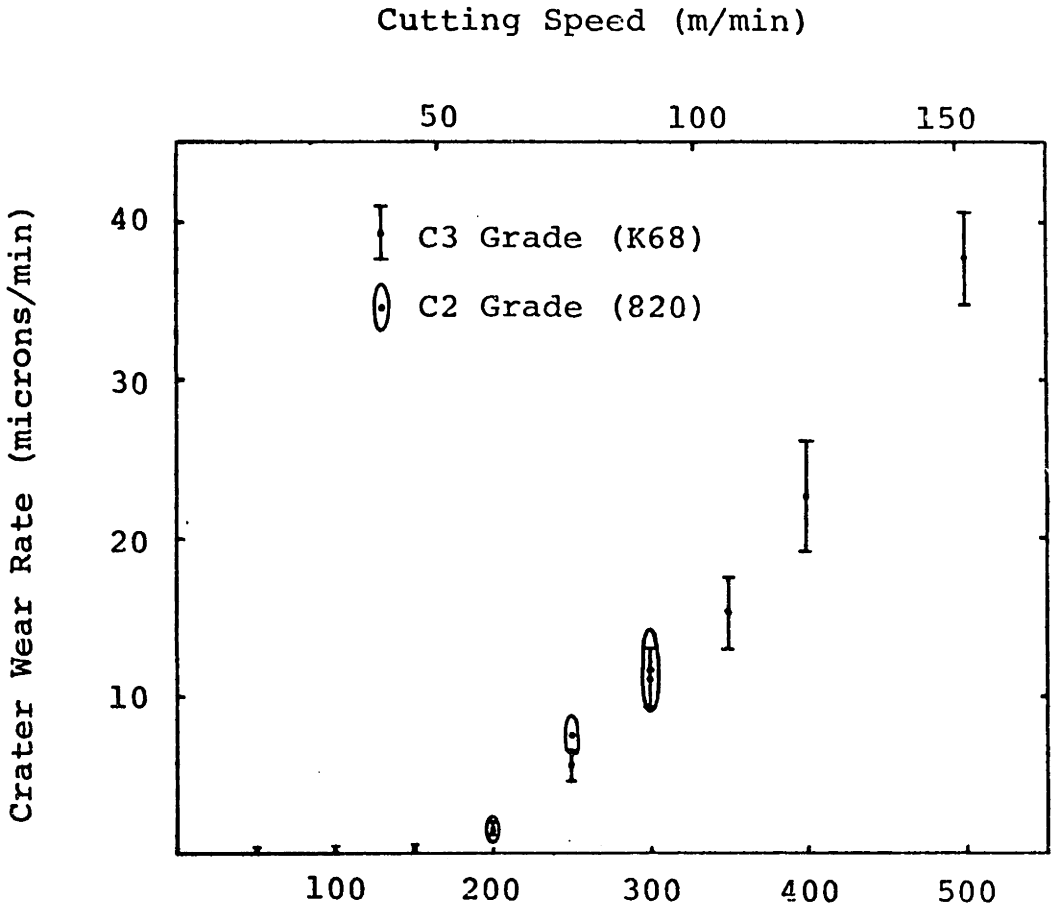

Figure 2. Wear Rate vs. Cutting Speed for C2 and C3 Carbide Grades Turning Ti 6Al-4V

Table 1 Cutting Tools Tested and Number of Tests Performed on Each

Tool Material	Supplier	Thickness (microns)	Substrate	Grade	# Tests on Ti 6Al-4V
Cemented WC	—	—	Kennametal K68	C3	43
"	—	—	Surftech H-25X	C2	3
"	—	—	Surftech H-2S	C3	1
"	—	—	Carboloy 820	C2	12
WC-based Complex Carbide	—	—	Kennametal K7H	C8	3
Cemented TiC	—	—	Ex-Cell-O XL88	—	3
TiC	Carboloy	5	Carboloy (WC)	C2	1
"	Quad Group	0.10	G.E. Compax**	—	5
HfC	Kramer	3-6	Kennametal K68	C3	4
"	Surftech	5	Surftech H-25X	C2	1
ZrC	Surftech	3	Kennametal K7H	C8	1
TiN	Teledyne	5	Firth Sterling TC+	C2	3
HfN	Teledyne	5	Firth Sterling HN+	C2	3
TiB_2	Raytheon	3.1-7.3	Kennametal K7H	C8	3
TiCN	—	—	Teledyne SD-3	—	2
CBN	—	—	G.E. Borazon	—	2
Diamond	—	—	G.E. Compax**	—	9
"	—	—	DeBeers Syndite**	—	5
Al_2O_3	—	—	General Electric	—	1
HfO_2	—	—	G.E. Al_2O_3	—	1
La_2O_3	—	—	M.I.T.	—	1

Notes: *These tools were coated at M.I.T. using a deposition process covered by U.S. Patent Number 4,066,821 issued to Cook and Kramer [60].

**These tool materials were brazed into the corners of cemented carbide inserts by Neuber Industrial Diamond Company.

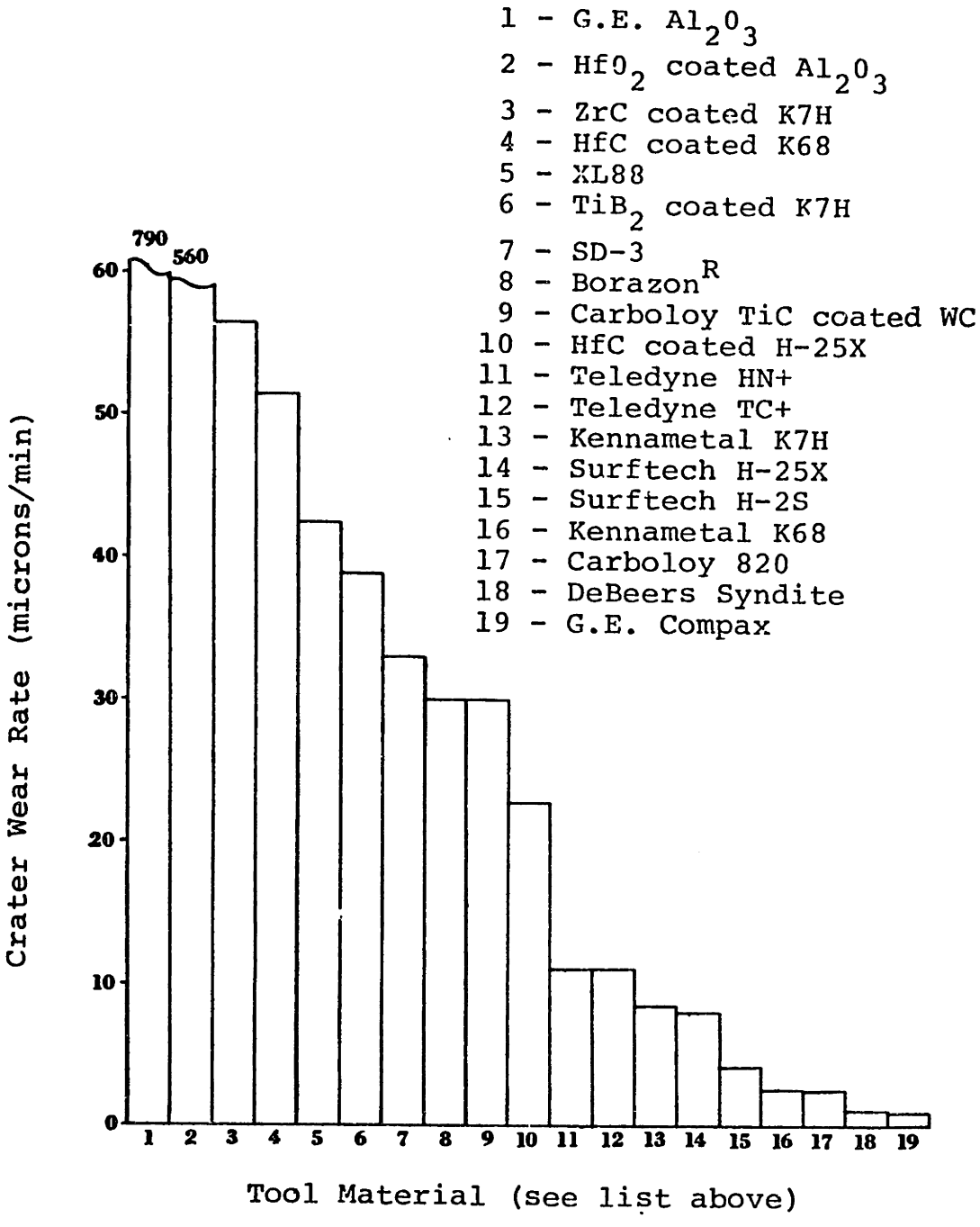

Figure 3. Bar Graph of Average Crater Wear Rates of Various Tool Materials Turning Ti 6Al-4V at 200 sfpm (61.0 m/min)

of 5(fpm (152 m/min), 1000 sfpm (305 m/min) and 1500 sfpm (475 n) with W-Al_2O_3 (W.R. Grace and Co.) and Al_2O_3-TiC (Gree f) cermet materials. These inserts failed catastrophically lowing very rapid cratering at 500 sfpm (152 m/min) and at th gher speeds the inserts failed immediately.

VI. High Speed Tests

A st was performed on C 130AM titanium alloy with Boraz at 1000 sfpm (305 m/min). At this cutting speed a strai continuous chip was formed and sparking occurred. The t cratered rapidly and failed in 15 sec. with a crater depth excess of 50 microns.

A cutting speed of 1500 sfpm (457 m/min) on Ti 6Al-4V, the cr r wear rate of Borazon^R (CBN) was measured to be over 5 microns/min, which limits the tool life to approximately ive seconds (see Figure 4).

P crystalline diamond tools (Syndite^R and Compax^R) were t ed at 1000 sfpm (305 m/min) and 1500 sfpm (457 m/min), but th ear rate at these speeds could not be measured due to fai e of the braze which holds the material to its base.

A speeds from 1000 to 2000 sfpm (305 to 610 m/min) C3 grade ented WC tools (K68) failed within seconds due to gross stic deformation of the cutting edge and chip welding wa ommon to most cuts. The crater wear rate varied from a oximately 270 microns/min at 305 m/min to approximately 500 microns/min at 610 m/min.

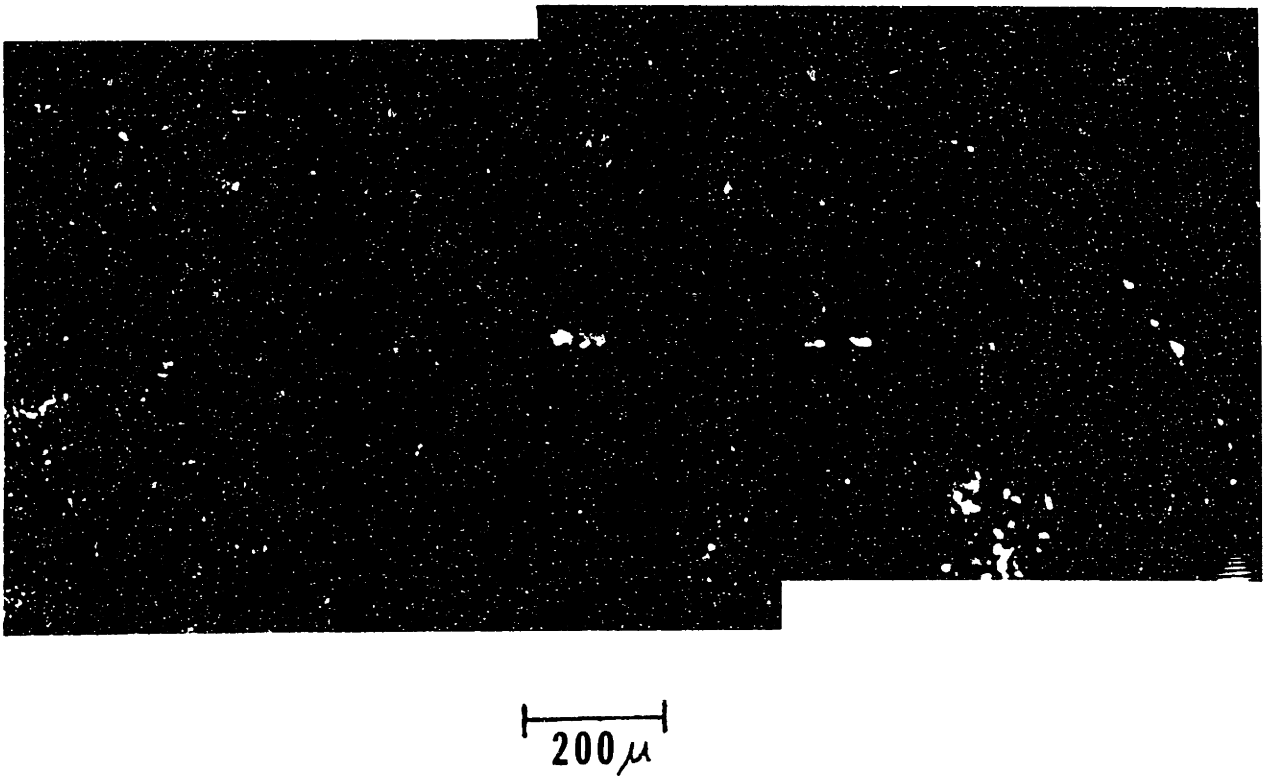

Figure 4 Micrograph of Borazon^{R} (CBN) after 4.5 seconds of Turning Ti 6Al-4V at 1500 sfpm (457 m/min), .005 ipr (.127 mm/rev).

Common to all cuts at speeds greater than 1000 sfpm (305 m/min) was the formation of a straight chip, as opposed to the coiled chip obtained at lower cutting speeds.

VII. Analysis of the Tool Wear Mechanism in the Machining of Titanium Alloys

In the turning of Ti 6Al-4V at cutting speeds ranging from 200 sfpm (61.0 m/min) to 400 sfpm (122 m/min) crater wear limits the tool life of cemented tungsten carbide tooling. Flank wear is stable and doesn't contribute to tool failure until plastic deformation of the cutting edge causes acceleration of the wear at the flank. At speeds in the range of 400 sfpm (122 m/min) to 2000 sfpm (610 m/min), this deformation becomes pronounced. At speeds between 200 sfpm (61.0 m/min) and 300 sfpm (91.4 m/min) the best tungsten carbide grade tested (K68, C3) failed by cratering with less than .005 in. (0.13 mm) of flank wear and very little plastic deformation at the time of failure by edge breakdown. Figure 5 shows the rake face and flank of a Kennametal K68 (C3 grade) tool after machining Ti 6Al-4V at 200 sfpm for 10 min. The crater depth in the center of the crater is about 23 microns and only 10% of the flank wear exceeded .004 in. (0.1 mm). Adherent titanium makes the flank wear look worse than it really was, since the same tool showed less apparent wear on the flank after 20 minutes of cutting. From experience, tools generally fail by

CRATER

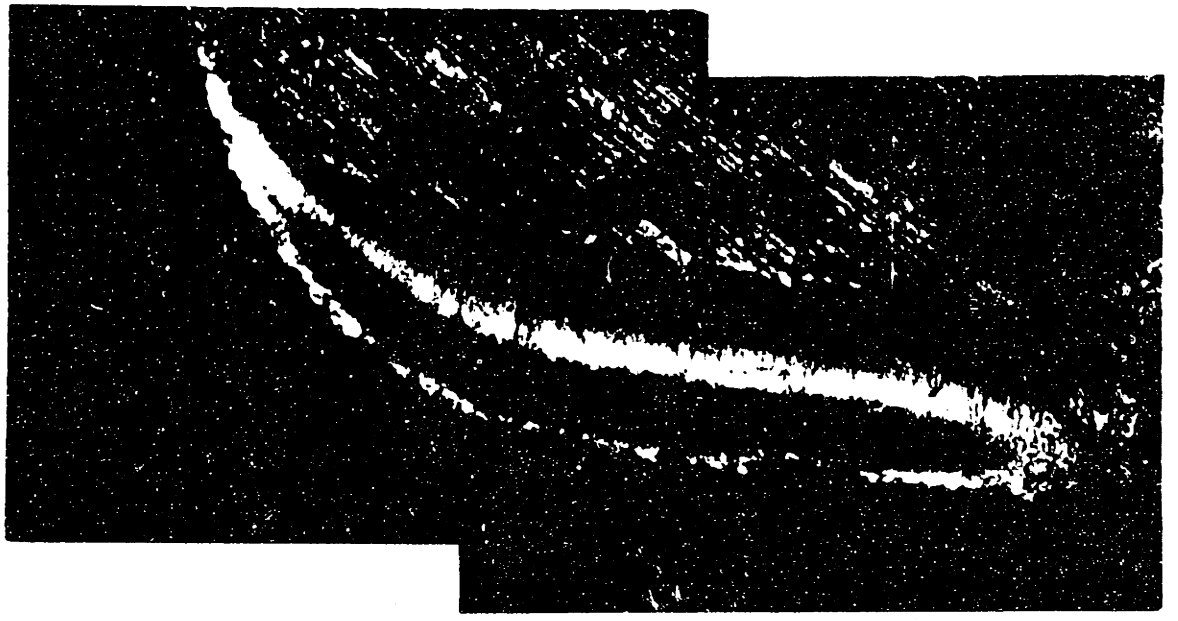

200μ

FLANK

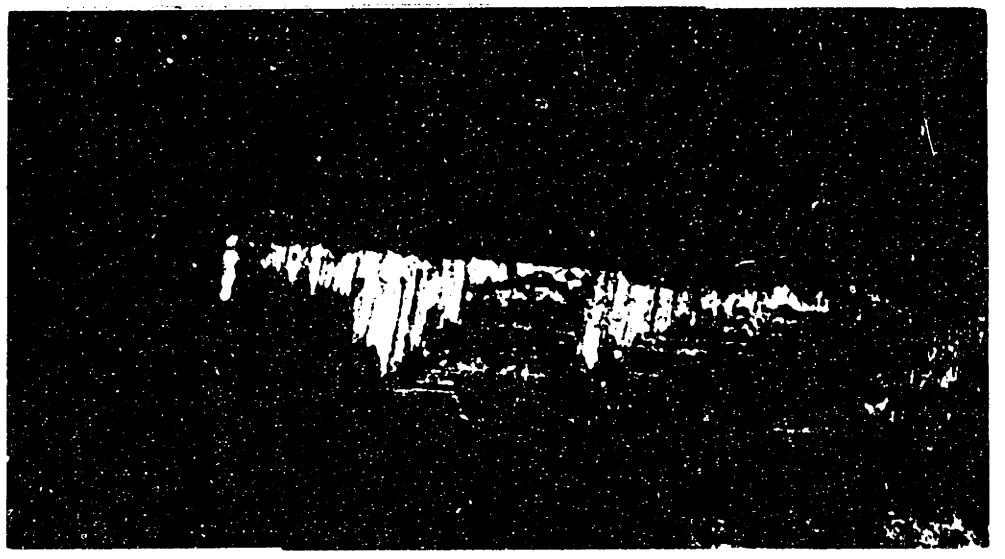

Figure 5. K68 after 10 minutes of cutting at 200 SFPM (61.0 M/MIN)

cratering when the crater depth reaches about 50 microns, causing the cutting edge to break down, whereas about .030 in. (0.76 mm) of flank wear is necessary to cause tool failure.

A. Crater Wear in the Machining of Steel and Nickel-Based Alloys

In the machining of steel and nickel based alloys near the limit of application of cemented carbide tooling, crater wear predominates. In this high speed range, it has been shown that crater wear results from the chemical dissolution of the tool material in the material being cut [63, 64]. The fact that titanium carbide additions to tungsten carbide-based tools increase the wear resistance of these tools in the machining of steel is due to the low solubility of TiC in steel.

Since crater wear is the dominant form of tool wear in the machining of titanium alloys, my first assumption was that the tool wear might be explained by a chemical dissolution model. This assumption, although it was eventually shown to be invalid, led us to consider a broad range of possible explanations for the wear of cutting tools in titanium machining. Predictions of relative rates of wear based on these mechanisms were compared with experimental results. Results are summarized in the following sections.

B. Solution Wear Theory

If the wear of a tool material proceeds by diffusion, the flux of tool material into the chip may be expressed as [63]:

$$Vwear = K \left[-D\frac{dc}{dy} + CV_y\right]_{y=0} \quad (1)$$

where: c = the concentration of the tool material

V_{wear} = the wear rate of the tool material

K = the ratio of the molar volumes of the tool material and the work material

D = the diffusion coefficient of the slowest diffusing tool constituent in the work material

C = the solubility of the tool material in the work material

Vy = the bulk velocity of the chip material at the tool/chip interface perpendicular to the interface.

The first term in the equation is the diffusion flux, with the driving force for diffusion being the concentration gradient. In the machining of steel and nickel-based alloys this term is insignificant compared to the second term, which is a bulk flow term resulting from the slowing down of the chip as it passes over the tool/chip contact area [63, 64].

If the mechanics of chip flow are assumed to be similar for different tool materials cutting under identical conditions, the relative wear rates of the tool materials may be taken as the ratio of the products of the solubility and the molar volume for each material [64]:

$$\text{Relative Wear Rate} = \frac{V_{\text{wear 1}}}{V_{\text{wear 2}}} = \frac{V_1 C_1}{V_2 C_2} \qquad (2)$$

where:

$V_{\text{wear i}}$ = the wear rate of tool material i

V_i = the molar volume of tool material i

C_i = the equilibrium concentration (solubility) of tool material i in the work material at the cutting temperature

The molar volumes of many tool materials are available in the literature, and are easily estimated from molecular weight and density information or from lattice parameter measurements.

Solubility of a tool material in a workpiece material is dependent on both the chemical stability of the tool material, and the affinity of its constituent elements for the workpiece material at the cutting temperature. High temperature solubility data is scarce and is difficult to measure. In general, solubilities have to be estimated from thermochemical data on the materials of interest. The solubility of a tool material in a workpiece material can be expressed in terms of the free energy of formation (stability) of the tool material and the excess free energies of solution (affinity) of the tool constituents at the cutting temperature, T. The method for estimating the solubility of tool materials is described in Appendix A, and

estimated solubilities are given in Table A2.

The solubilities calculated in Appendix A and listed in Table A2 do not explain the high wear rates of HfC and ZrC coated tools relative to that of WC (see Figure 3). The least soluble material tested, La_2O_3, was not tough enough to withstand the cutting forces, so wear data could not be obtained.

Figure 6 shows the rake face of an HfC coated tool next to its uncoated cemented WC substrate Kennametal K68 (C3), after both tools have turned Ti 6Al-4V for 30 sec. at 200 sfpm (61.0 m/min). The uncoated tool has an adherent layer of titanium over its whole crater and shows less than 1.5 microns of crater wear. On the other hand, the HfC coated insert shows between 28 and 34 microns of wear on the rake face, and the coating is only 6 microns thick. The fact that the coated tool wore at about 20 times the rate of the identical uncoated tool can not be due to the different solubilities of the two materials, since, if anything, HfC should be less soluble in titanium. Tests revealed that even when the HfC coating was completely penetrated during the cut, the coated tools still continued to wear at a greater rate than the uncoated tools. It appears as if the wear mechanism in the machining if titanium is fundamentally different from that in the machining of steel and nickel alloys. Therefore, it is necessary to examine other

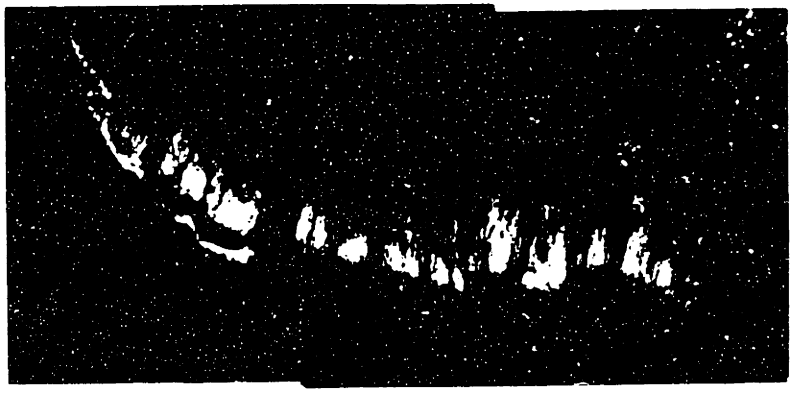

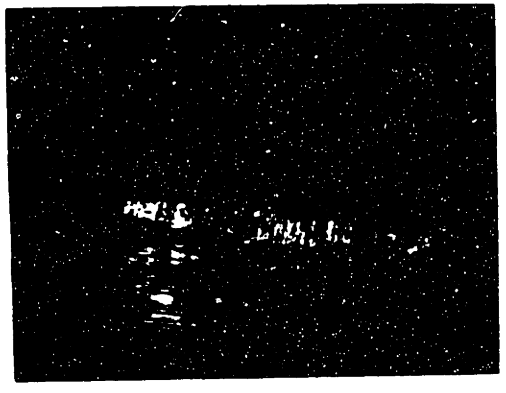

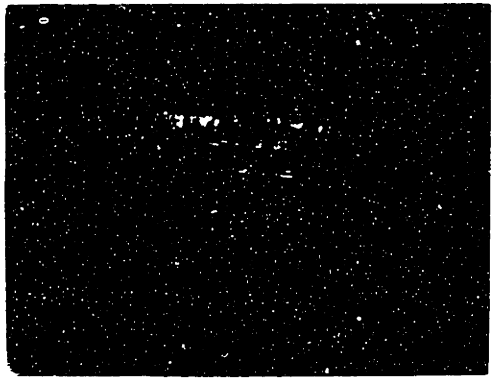

Figure 6. Comparison of Uncoated and HfC Coated WC Tools After Turning Ti 6Al-4V Under the Same Conditions

possible explanations for the observed behavior.

C. Influence of Cutting Temperature on Wear

Since any chemical wear mechanism would be affected by changes in the cutting temperature, if the cutting temperature were much higher for the coated tools than for the uncoated tools, for some reason, an increase in wear rate of the coated tools over that of the uncoated tools might be expected. However, cutting temperature measurements taken on TiB_2 and HfC coated conditions indicated that there is very little difference in cutting temperatures between coated tools and their uncoated substrates. In fact, the average cutting temperature for the HfC coated K68 (C3) inserts, 1010°K, was 60°K lower than that of the uncoated K68 (C3) inserts, 1070°K, at 200 sfpm (61.0 m/min). Also, the variation in solubility with temperature is not very large, and shouldn't account for the discrepancy.

Cutting temperatures were measured while machining with Kennametal K68 (C3) cemented WC at speeds from 50 to 2000 sfpm (15.2 to 610 m/min). Figure 7 is a plot of measured cutting temperature vs. cutting speed for this material. As can be seen in the plot, the average cutting

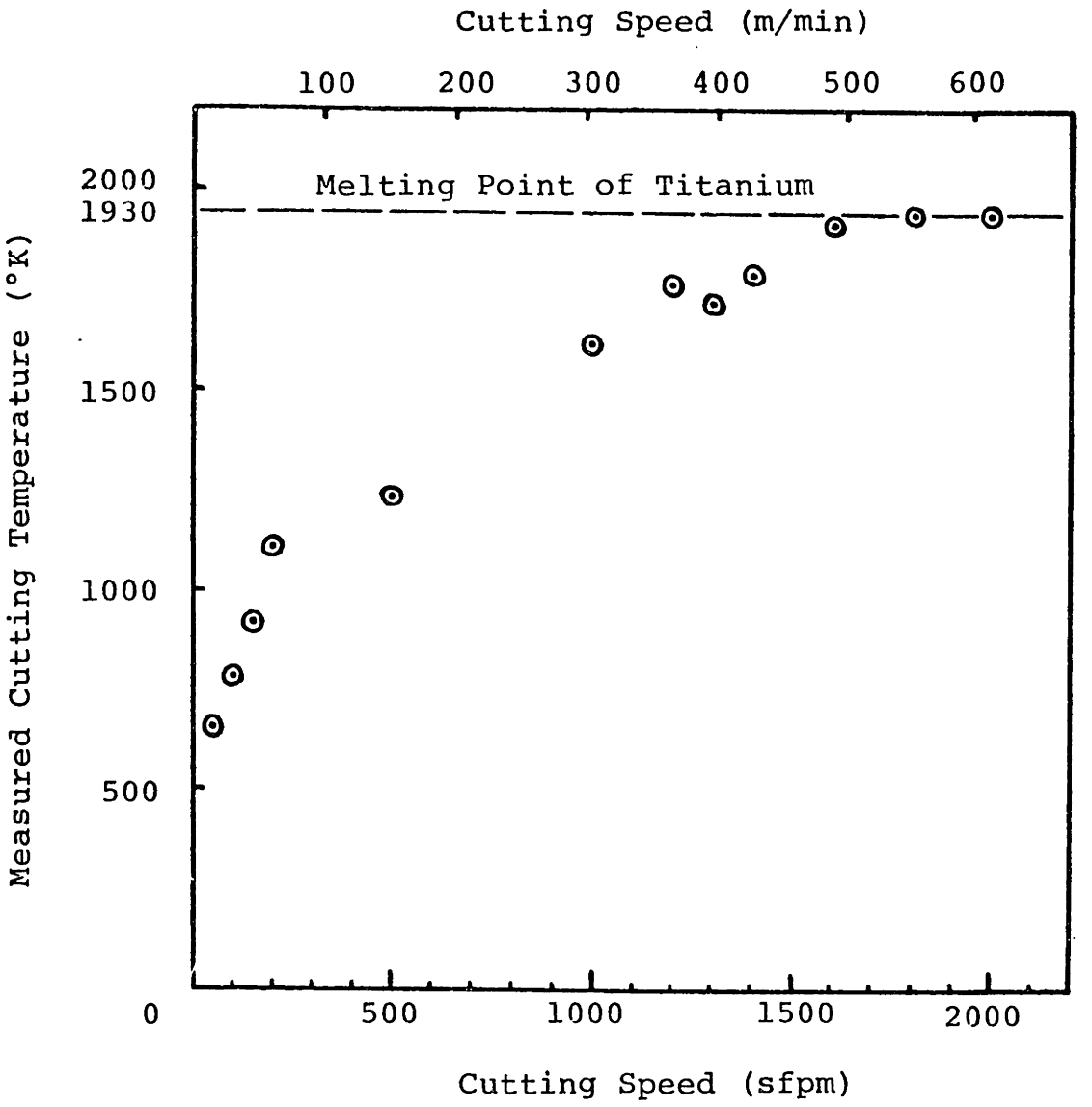

Figure 7. Plot of Average Cutting Temperature vs. Cutting Speed for K68 Turning Ti 6Al-4V

temperature asymptotically approaches the melting point of titanium at higher cutting speeds. At lower speeds it is believed that the maximum cutting temperature at the center of the crater may be a fair amount higher than the average cutting temperature [65]. As the cutting temperature approaches the melting temperature of the metal being cut, the temperature gradient across the rake face of the tool may be reduced, and the heat more evenly distributed.

Based on the results shown in Figure 7, the analyses of tool wear were carried out for temperatures in the range of 1300 - 1500°K, the estimated maximum cutting temperature.

D. Solubility of the Least Soluble Component

If the wear of cutting tool materials in the machining of titanium proceeds by dissolution of the tool materials in titanium, then it seems reasonable that the solubility of the tool material will be limited by the solubility of the least soluble component. That is, if tungsten carbide is being employed as a tool material, and since the solubility of tungsten in titanium is much greater than that of carbon, the solubility of WC will be no greater than the solubility of C.

Table 2 lists the solubilities of the tool constituents in titanium obtained from phase diagrams. Comparison of Table 2 with Table A2 reveals that all of the tool materials except for HfN, HfO_2 and La_2O_3 have predicted solubilities

Table 2 Solubilities of Tool Constituents in Titanium

Tool Constituent	Solubility (at. %) 1300°K	1400°K	1500°K	Reference
Al	15.0	19.0	28.0	[66]
B	1.0	1.0	1.0	[67]
C	0.6	0.6	0.6	[68]
Hf	*	*	*	[66]
La	*	*	*	[66]
N	23.6	23.5	23.2	[68]
Nb	*	*	*	[69]
O	34.0	34.0	34.0	[68]
Si	2.2	3.0	4.0	[66]
Ta	*	*	*	[68]
Ti	100	100	100	
V	*	*	*	[68]
W	*	*	*	[66]
Zr	*	*	*	[66]

*These constituents are soluble over a wide range of concentrations and temperatures.

in titanium which are greater than at least one of their constituents. In all of these cases the solubility of the tool material should be best approximated by the solubility of the least soluble component divided by the number of atoms of that component per molecule of tool material.

Since the solubility of titanium in itself is 100%, the solubility of titanium containing tool materials would be limited by the solubility of the other tool constituents in titanium. Therefore, the hard titanium compounds provide an ideal system to test this hyposthesis. The three titanium containing tool materials available for testing are TiC, TiN and TiB_2.

Both carbon (C) and boron (B) have solubilities in titanium of less than 1 atomic % at temperatures up to around 1900° and 1800°K respectively [66]. Nitrogen (N) has a solubility of over 21 at % at temperatures over 1323°K [68]. If the solubility of the least soluble component in titanium controlled the wear of these cutting tool materials, then TiN would be the least wear resistant of the three materials. However, test results at 200 sfpm (61.0 m/min) indicate that TiN, with a crater wear rate of about 10 microns/min is actually 3 to 4 times more wear resistant than TiB_2 and TiC, which seem to have nearly the same crater wear rate of about 40 microns/min. Like the HfC coated tools, these tools had problems with irregular wear and coating delamination, particularly in the case of the TiB_2 coated tools, as is shown in Figure 8.

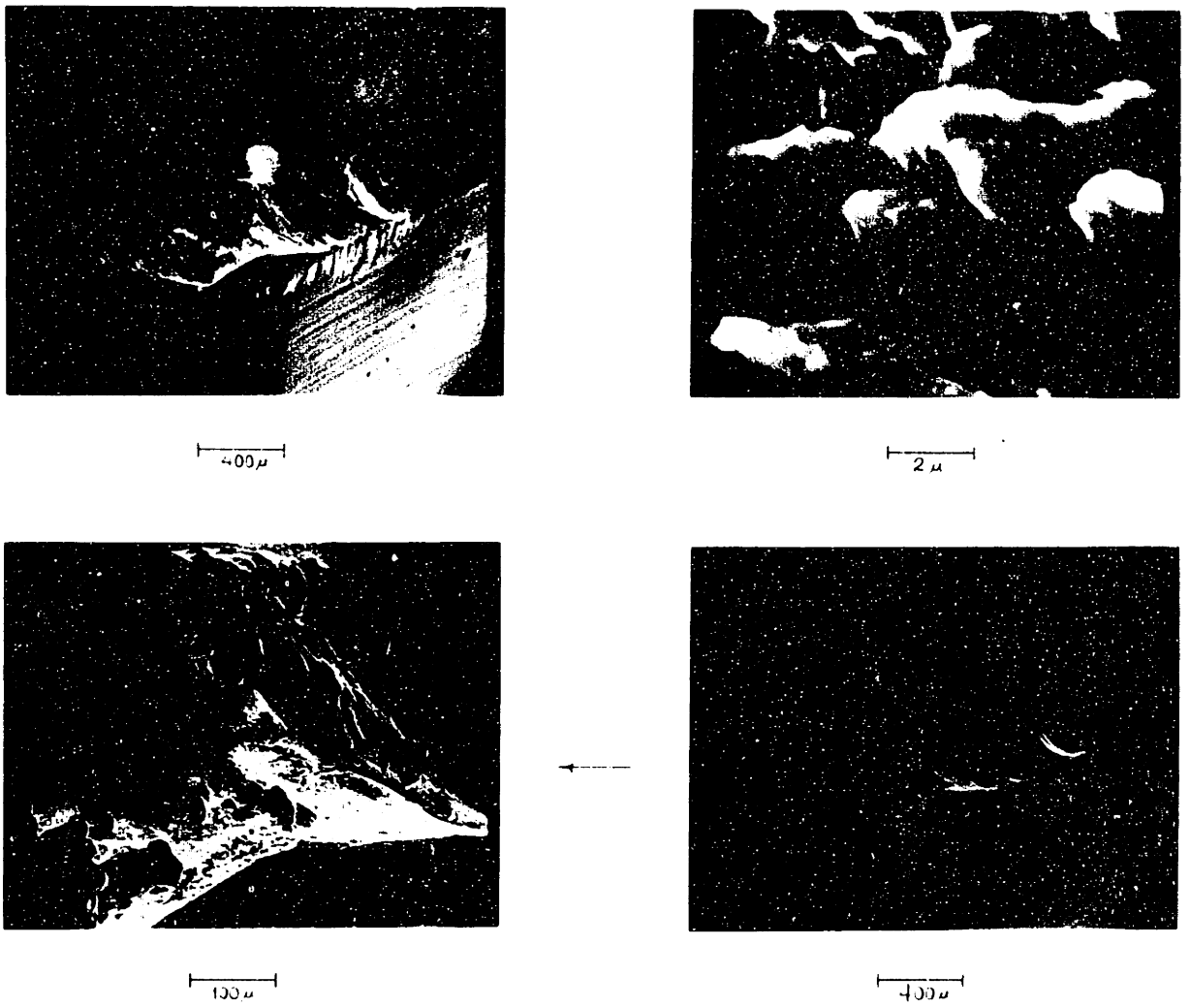

Figure 8. SEM Photos of TiB_2 Coated WC Based Tool Showing Coating Delamination

E. Upper Bound Model For Diffusion Flux

Cook and Nayak [70] have modelled the cutting process with the assumption that no deformation occurs in the chip as it slides across the tool/chip interface. This model eliminates the bulk flow term in Equation 1 and maximizes the wear due to diffusion.

The predicted wear rate in the center of the crater from this model is:

$$V_{wear} = -KC\sqrt{\frac{D}{\pi t}} \qquad (3)$$

where

V_{wear} = the wear rate of the tool material

K = the ratio of molar volumes of the tool and chip materials

C = the equilibrium concentration of the tool material in the chip

D = the diffusion coefficient of the slowest diffusing tool constituant in the chip

t = the time it takes for the chip to move from the edge of the tool to the center of the crater

The diffusion coefficients of some tool constituent materials in titanium were calculated from activation energy and frequency factor data given in the literature using the equation:

$$D_T = D_o e^{-Q/RT} \quad (4)$$

where:

D_T = the diffusion coefficient

D_o = the frequency factor

Q = the activation energy

R = molar gas constant

T = temperature

The diffusion coefficients, calculated at 1300, 1400 and 1500°K are listed in Table 3.

The time required for the chip to slide from the tool edge to the center of the crater is equal to:

$$t = \frac{d}{V_c} \quad (5)$$

where:

d = the distance from the edge of the tool to the center of the crater

V_c = the chip velocity

The chip velocity is equal to the product of the cutting speed and the ratio of the depth of cut to the chip thickness (chip thickness ratio).

At 200 sfpm (61.0 m/min) and a depth of cut of .050 in (1.27 mm) the chip thickness was measured by micrometer to be approximately .008 in (0.2 mm), which gives a chip velocity of 635 cm/sec. The distance from the edge

Table 3 Diffusion Coefficients of Some Tool Constituents in Titanium

Solute (tracer) in B-Ti	Activation Energy, Q, Kcal/mole	Frequency factor, D_o ($\frac{cm^2}{sec}$)	D_T (Diffusion Coefficient) ($\frac{cm^2}{sec}$) 1300°K	1400°K	1500°K
C^{14}[71]	20.0	3.2×10^{-3}	1.3114×10^{-6}	2.2799×10^{-6}	3.6817×10^{-6}
Co^{60}[71]	30.6	1.2×10^{-2}	8.6085×10^{-8}	2.0062×10^{-7}	4.1766×10^{-7}
	52.5	2.0	2.9861×10^{-9}	1.2750×10^{-8}	4.4863×10^{-8}
Mo^{99}[71]	43.0	8.0×10^{-3}	4.7232×10^{-10}	1.5509×10^{-9}	4.3459×10^{-9}
	73.0	20	1.0685×10^{-11}	8.0422×10^{-11}	4.6247×10^{-10}
Nb^{95}[71]	39.3	5.0×10^{-3}	1.2363×10^{-9}	3.6648×10^{-9}	9.3982×10^{-9}
	73.0	20	1.0685×10^{-11}	8.0422×10^{-11}	4.6247×10^{-11}
V^{48}[71]	32.2	3.1×10^{-4}	1.1971×10^{-9}	2.9160×10^{-9}	6.3080×10^{-9}
	57.2	1.4	3.3890×10^{-10}	1.6479×10^{-9}	6.4895×10^{-9}
W^{185}[71]	43.9	3.6×10^{-3}	1.5002×10^{-10}	5.0501×10^{-10}	1.4460×10^{-9}
Zr^{95}	35.4	4.7×10^{-3}	5.2590×10^{-9}	1.3995×10^{-8}	3.2688×10^{-8}
Ti^{44}[71]	31.2	3.58×10^{-4}	2.0359×10^{-9}	4.8241×10^{-9}	1.0188×10^{-8}
	60.0	1.09	8.9259×10^{-11}	4.6896×10^{-10}	1.9749×10^{-9}
N[72]	33.8	3.5×10^{-2}	7.9112×10^{-8}	2.0022×10^{-7}	4.4773×10^{-7}
O[72]	48.2	1.6	1.4222×10^{-8}	5.3463×10^{-8}	1.6844×10^{-7}

of the tool to the center of the crater, obtained from crater traces, was approximately 0.02 cm. Using Equation 5, t was calculated to be 3.15×10^{-5} sec.

The molar volume of titanium is 10.64 cm^3/mole [73]. the predicted wear rates of various potential tool materials, calculated at 1400°K using Equation 3, are contained in Table 4. The diffusion coefficients were taken from Table 3. The equilibrium concentrations were obtained from Tables 2 and A2, and were assumed to be equal to the solubility of the least soluble component in cases where the solubility is greater than the solubility of the least soluble component.

This model overestimates the wear rate of tool materials in the machining of titanium and does not account for the large velocity gradients which must be present in the chip flow geometry.

F. Abrasive Wear of Cutting Tools

Ramalingam [75] attributes the wear of carbide tools, in the machining of steel with hard inclusion particles, including the crater wear, to abrasive mechanisms. This is particularly clear in the case of machining of high silicon content aluminum, where Si particle inclusions cause most tool materials to wear at a rapid rate. It has been found that even relatively soft abrasives, less than 1.2 times as hard as the material being abraded, can cause wear to occur [76, 77].

Table 4 Predicted Wear Rates From Upper Bound Diffusion Model (at 1400°K)

Tool Material	Ratio of Molar Volumes K [73]	Slowest Diffusing Component	Diffusion Coefficient (cm^2/sec)	Solubility (mol. %)	Predicted Wear Rate (cm/sec)	(μ/min)
Diamond	.3214	C	2.2799×10^{-6}	0.6	2.93×10^{-4}	176
HfC	1.2641	C*	2.2799×10^{-6}	0.6	1.15×10^{-3}	691
NbC	1.2660	Nb	3.6648×10^{-9}	0.6	4.62×10^{-5}	27.7
SiC	1.1720	C*	2.2799×10^{-6}	0.6	1.07×10^{-3}	640
TaC	1.2509	C*	2.2799×10^{-6}	0.6	1.14×10^{-3}	684
TiC	1.1466	Ti	4.8241×10^{-9}	0.6	4.80×10^{-5}	28.8
VC	1.0254	V	2.9160×10^{-9}	0.6	3.34×10^{-5}	20.0
WC	1.1654	W	5.0501×10^{-10}	0.6	1.58×10^{-5}	9.48
ZrC	1.4718	Zr	1.3995×10^{-8}	0.6	1.05×10^{-4}	63.0
BN	0.6701	N*	2.0022×10^{-7}	1.	3.01×10^{-4}	180.8
HfN	1.3111	N*	2.0022×10^{-7}	12.8	7.55×10^{-3}	4529
Si_3N_4	3.833	N*	2.0022×10^{-7}	1.0	1.72×10^{-3}	1035
TiN	1.0799	Ti	4.8241×10^{-9}	23.5	1.77×10^{-3}	1063
Al_2O_3	2.404 [71]	O*	5.3463×10^{-8}	7.5	4.19×10^{-3}	2514
HfO_2	1.957 [71]	O*	5.3463×10^{-8}	14.67	6.67×10^{-3}	4004
La_2O_3	4.702 [71]	O*	5.3463×10^{-8}	0.076	8.31×10^{-5}	49.84
ZrO_2	2.0677	Zr	1.3995×10^{-8}	17.0	4.18×10^{-3}	2508
TiB_2	1.4915 [74]	Ti	4.8241×10^{-9}	0.5	8.87×10^{-5}	53.21

*In these cases, the diffusion coefficients of the other (and in most cases the slowest diffusing) constituent was not available, so these are overestimates and may not be valid.

If abrasion by hard inclusions in titanium alloys (TiN, TiC, TiO, etc.) controlled the wear of tool materials in the machining of titanium, carbides would be much more susceptible to this type of wear than hard, abrasion resistant materials such as polycrystalline CBN and diamond. However, test results show that Borazon^{R} (CBN) has a much higher wear rate than both polycrystalline diamond and cemented WC in the machining of Ti 6Al-4V (see Figure 9). Since CBN is harder than any hard inclusions in titanium alloys, its high wear rate cannot be attributed to an abrasive mechanism.

G. The Wear of Polycrystalline Diamond In the Machining of Titanium Alloys

Because of its low wear rate relative to all other tool materials tested, and the lack of information concerning it in the literature, the wear of polycrystalline diamond tools was carefully monitored in machining Ti 6Al-4V at 200 sfpm (61.0 m/min), to determine what might cause the low wear rate. Figure 10 through 13 show the wear on the rake face and flank of a Compax^{R} tool at short intervals of cutting time up until 20 minutes of cutting at 200 sfpm (61.0 m/min).

Profile traces across the rake face of the tool show no apparent wear up until a cutting time of 4 min. In the micrographs, an adherent layer of titanium appears to cover

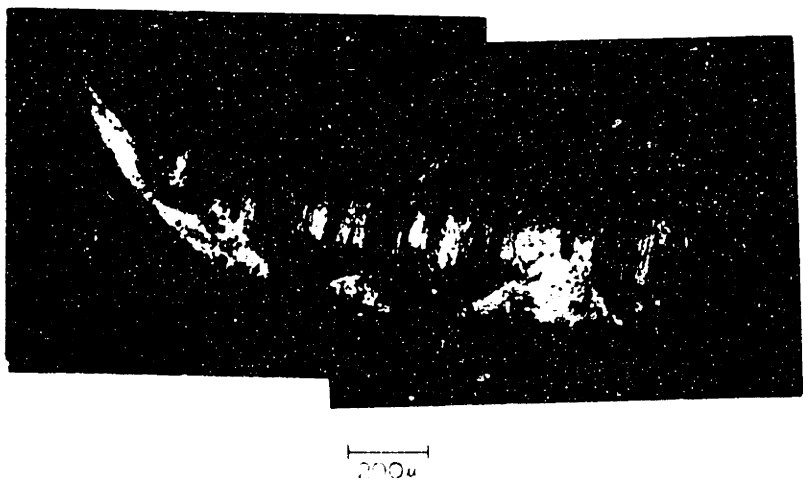

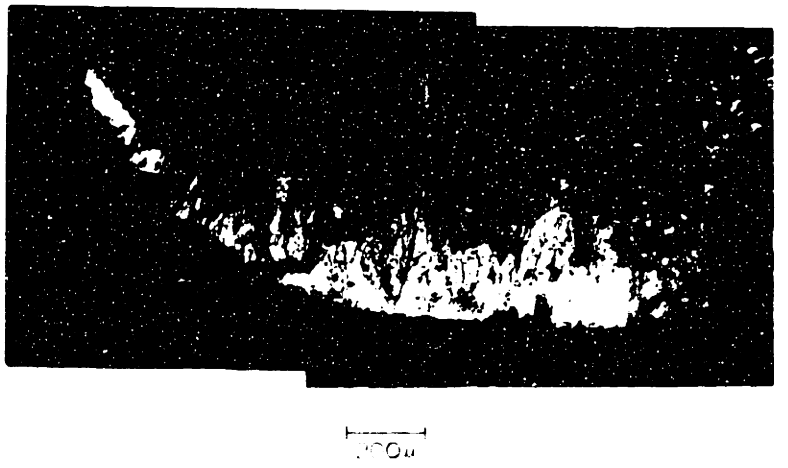

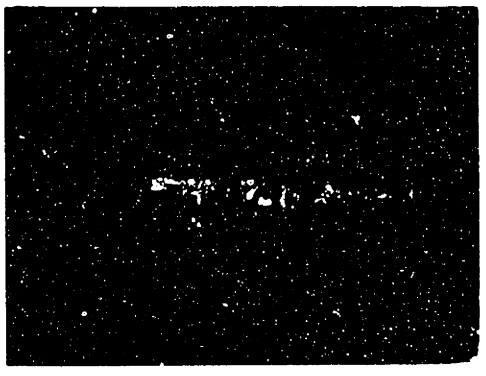

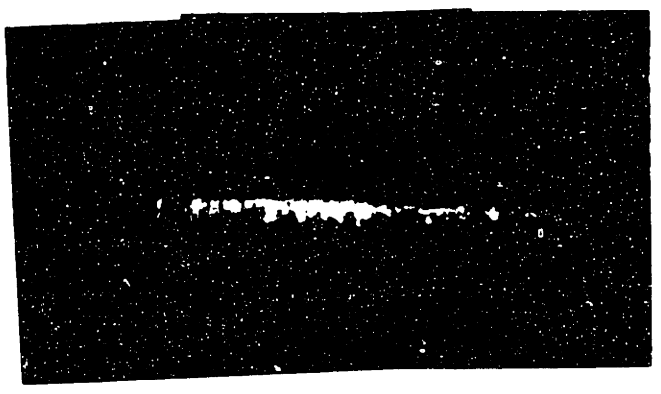

GE BORAZON SNG432
CUTTING SPEED: 200 SFPM (61 m/m.)
CUTTING TIME: 0.5 MIN.

G.E. COMPAX SNG432
CUTTING SPEED: 200 SFPM (61 m/m.)
CUTTING TIME: 0.5 MIN.

Figure 9. Comparison of CBN and Diamond Tools After Turning Ti 6Al-4V Under Same Conditions

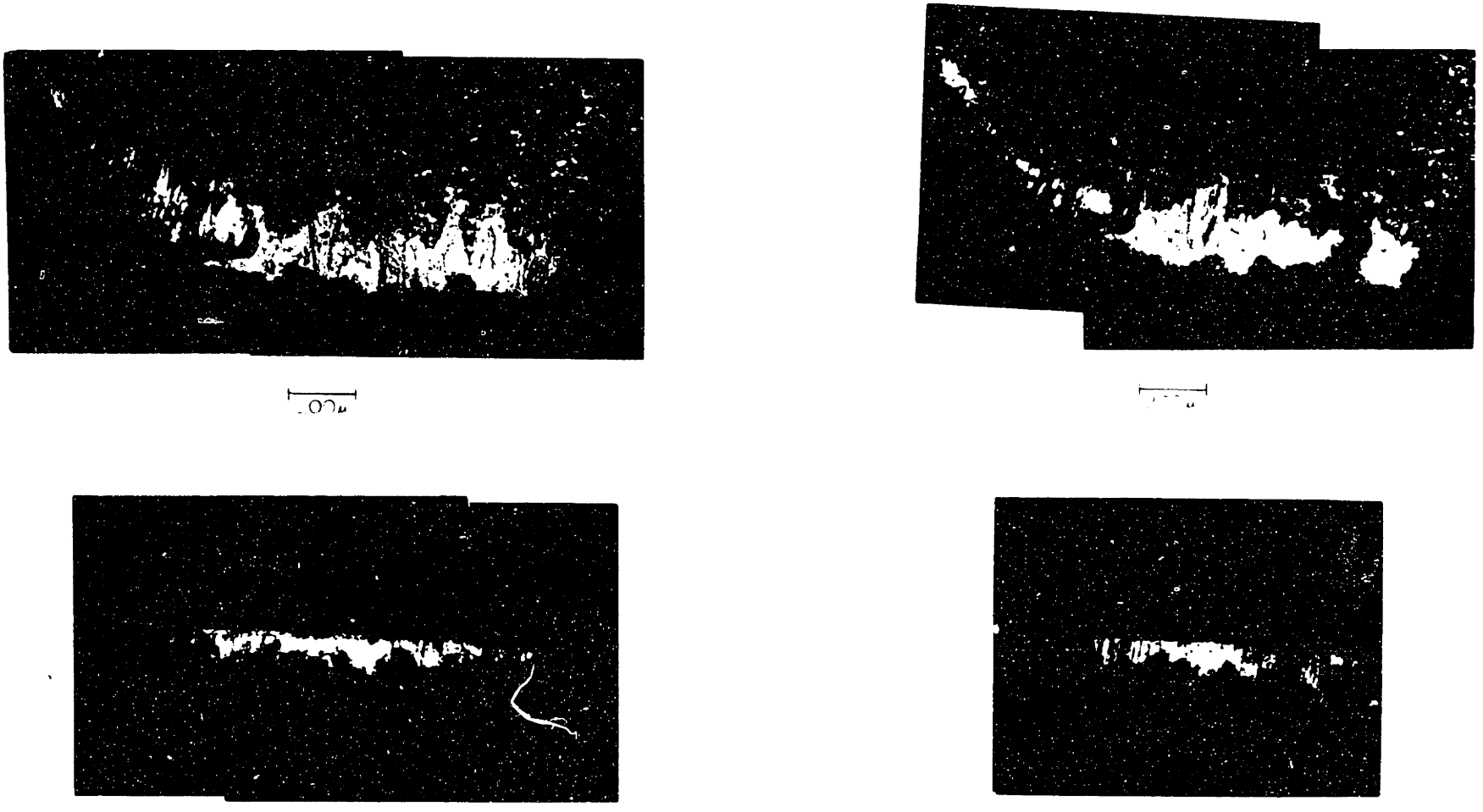

GE COMPAX SNG 432
CUTTING SPEED: 200 SFPM (61 m/min.)
CUTTING TIME: 1 MIN.

GE COMPAX SNG 432
CUTTING SPEED: 200 SFPM (61 m/min.)
CUTTING TIME: 2 MIN.

Figure 10. Micrographs of a Diamond Tool After Turning Ti 6Al-4V

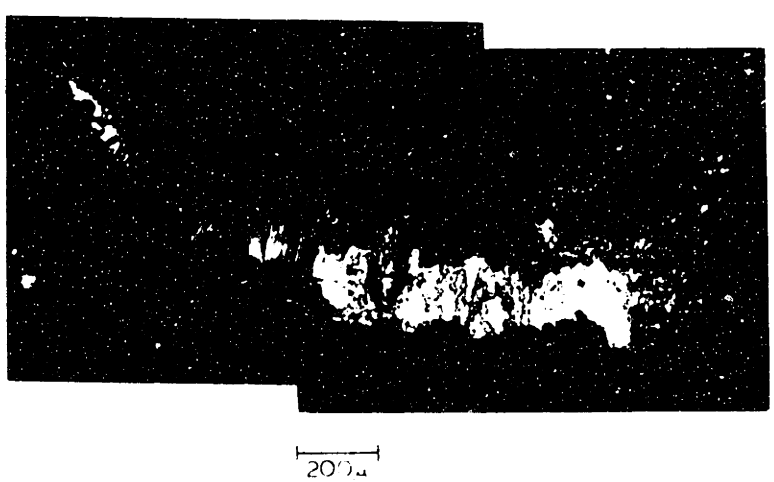

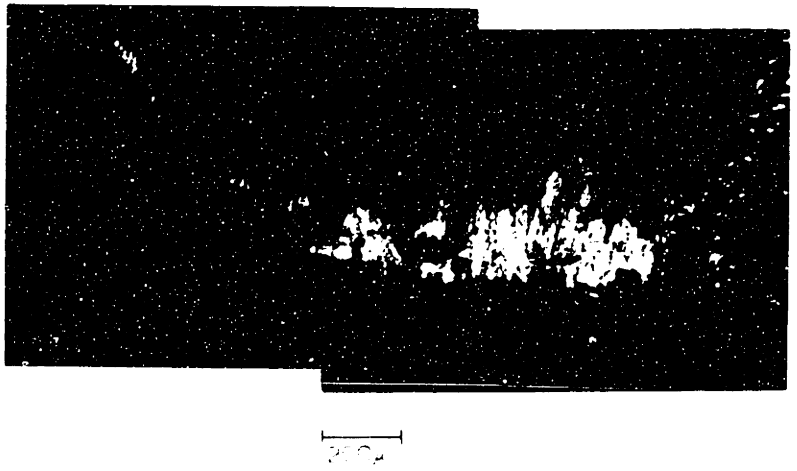

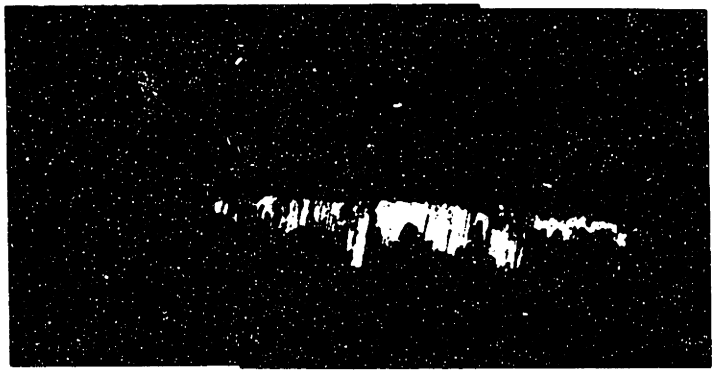

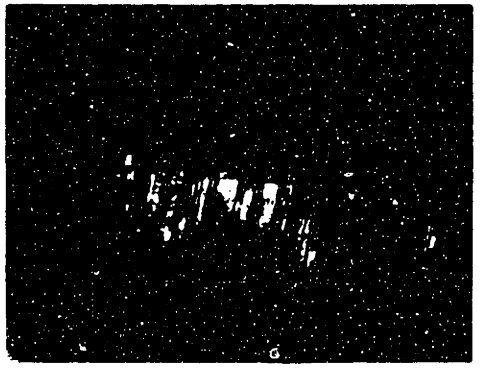

G.E. COMPAX SNG432
CUTTING SPEED: 200 SFPM (61 m/min.)
CUTTING TIME: 4 MIN.

G.E. COMPAX SNG432
CUTTING SPEED: 200 SFPM (61 m/min.)
CUTTING TIME: 4 MIN.

Figure 11. Micrographs of a Diamond Tool After Turning Ti 6Al-4V

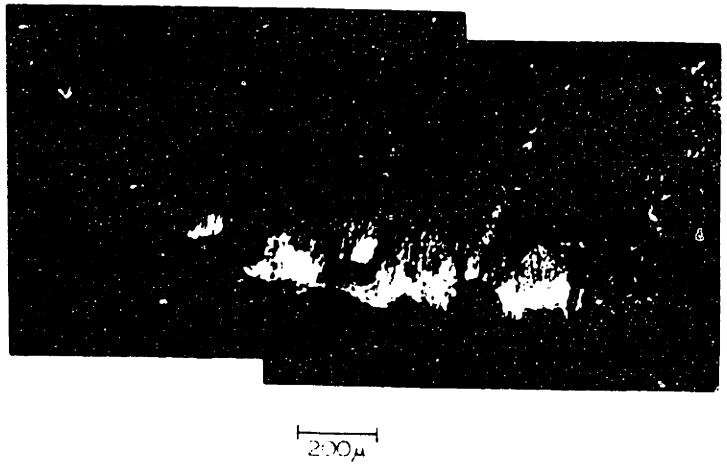

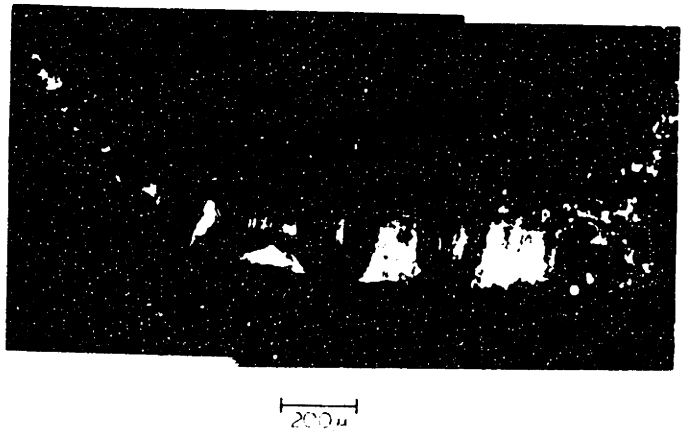

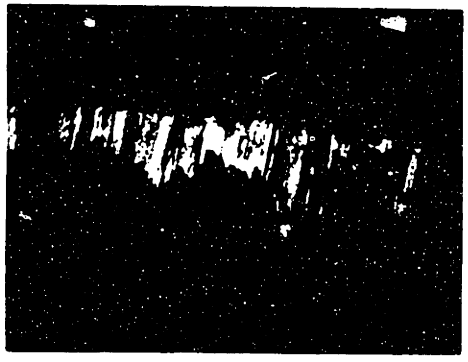

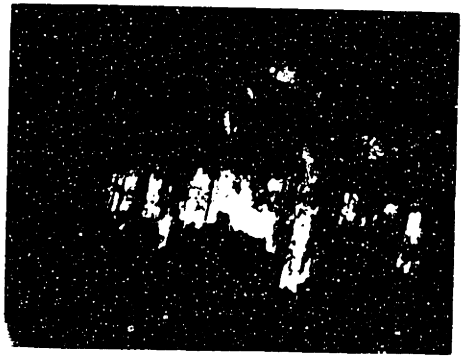

G.E. COMPAX SNG 432
CUTTING SPEED: 200 SFPM (61 m/min.)
CUTTING TIME: 10 MIN.

G.E. COMPAX SNG 432
CUTTING SPEED: 200 SFPM (61 m/min.)
CUTTING TIME: 15 MIN.

Figure 12. Micrographs of a Diamond Tool After Turning Ti 6Al-4V

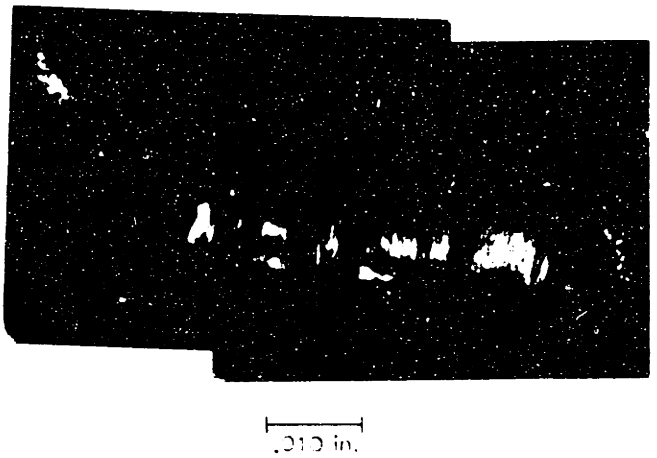

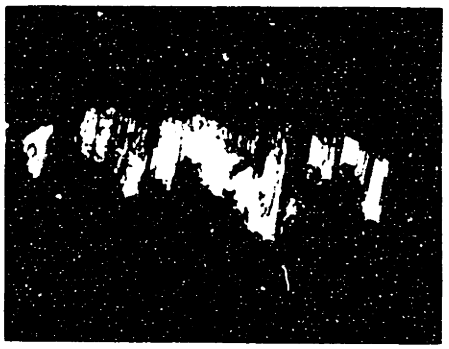

G.E. COMPAX SNG 432
CUTTING SPEED: 200 SFPM (61m/min.)
CUTTING TIME: 20 MIN.

Figure 13. Micrographs of a Diamond Tool After Turning Ti 6Al-4V

the surface. After 7 minutes of cutting, a zone of accelerated wear can be seen in the center of the "crater" area, which has a depth of approximately 7 microns. There is still no apparent wear over most of the rake face of the tool. After 15 minutes of cutting, three zones of accelerated wear are apparent on the rake face of the tool which show over 20 microns of wear, but still there are regions with essentially no wear. In the last 5 minutes of cutting, the previously unworn regions began to wear more rapidly. Flank wear proceeded at a fairly low rate, and after 20 minutes of cutting the wear land was less than .010 in. (.254 mm). Even though the crater and flank wear regions are starting to intersect in the regions of high wear, the surface finish was consistently excellent and the Compax^{R} tool was still cutting fine after 20 minutes.

The scalloped appearance of the rake face wear on the diamond tools is not unique to these tools, but can be seen quite clearly on the CBN and ZrC coated carbide tools (Figure 14). This effect is unusual and has not been discussed in the metal cutting literature. Uncoated cemented tungsten carbide tools do not show this discontinuous, scalloped form of wear when machining Ti 6Al-4V, but crater in a more conventional manner (Figure 15). Figure 15 shows the surfaces of cemented WC and polycrystalline CBN tools after etching the titanium from the surfaces with hydrofluoric acid for 20 min. The surface of the WC tool appears

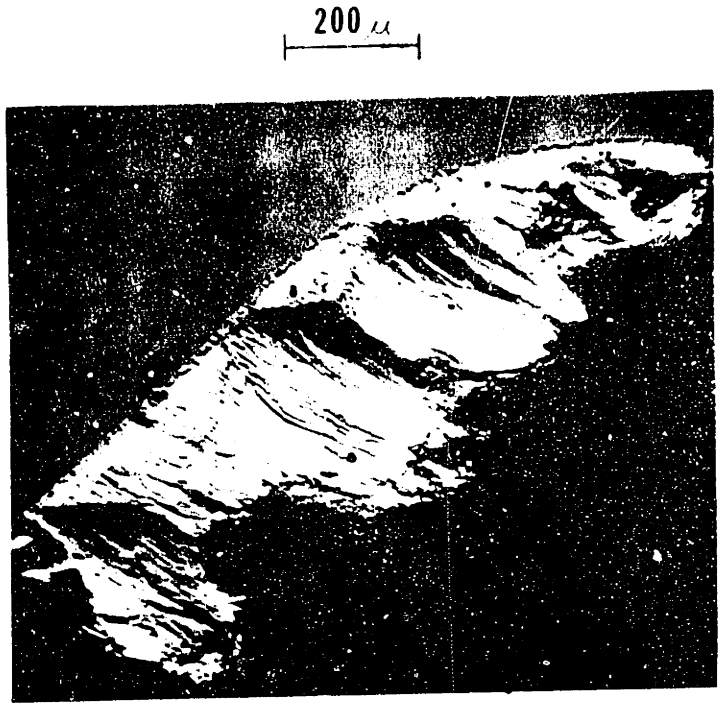

a Cutting Time: 0.5 minutes

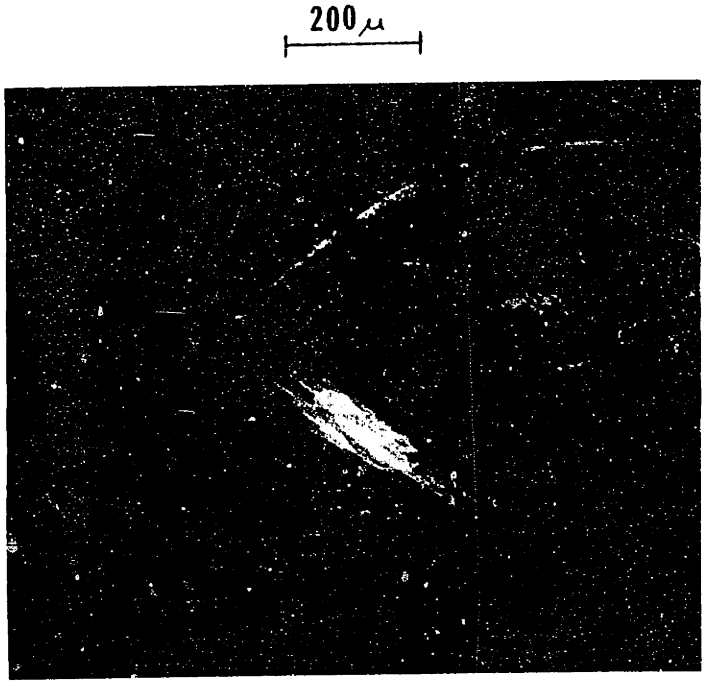

b Cutting Time: 1 minute

Figure 14. SEM Photos of a) CBN, and b) ZrC Coated K7H Tools Showing Scalloped Wear Pattern After Turning Ti 6Al-4V at 200 sfpm (61.0 m/min)

a

200 μ

b

Figure 15 Comparison of the Crater Surfaces of a) Cemented WC and b) Polycrystalline CBN Tools after Etching with HF for 20 Minutes.

to be chemically polished whereas the surface of the CBN tool is rough and appears to be abraded.

H. Interfacial Conditions Control the Wear

It is necessary to identify a mechanism by which rapid wear can occur in one region of the crater area while essentially no wear is present in an adjacent region which apparently is subjected to identical cutting conditions. Since crater wear occurs at the chip/tool interface, in order to account for the difference in wear rate, different regions of the rake area must be subject to different interfacial conditions during the cut. The chip formation process may be discontinuous, but the chip must be in contact with the tool over its width, due to the cutting forces present.

It is possible that, under certain conditions, titanium adheres to the tool and no relative sliding occurs at the tool/chip interface. A boundary layer of titanium forms at the interface, and only titanium on titanium sliding occurs. This would explain why essentially no wear occurs in certain regions of the crater area of some tools. In Appendix C an attempt is made to predict the boundary layer thickness and mass transfer rate assuming that sticking occurs at the interface.

Probably the most significant example is Borazon^{R} (CBN), which had essentially no wear in one region of its crater area, and a 30 micron deep pit in another (Figure 14a).

Tests on Inconel 718 with Borazon^{R} have shown that the wear of Borazon^{R} is very sensitive to interfacial conditions, with a wear rate at 135 sfpm (41.1 m/min) five times greater than at 600 sfpm (183 m/min).

It is not possible to see the tool/chip interface while the cut is in process, so it is necessary to look for signs of different boundary conditions on the tool surface after the cut is made.

VIII. Scanning Electron Microscope/Energy Dispersive Xray Analysis of Tool Wear

To determine what the worn and unworn areas of the tools look like at high magnification, to obtain Xray spectra of the elements present in these specific areas, and to obtain mappings of the location of the specific elements of interest which have been shown to be present on the tool, a scanning electron microscope (SEM) with an energy dispersive Xray analyser (EDS) was used.

An example of the use of the SEM/EDS system is given in Figure 16, which shows a HfN coated WC-based tool which has been analysed on a Cambridge SEM with a Kevex Model 550 Energy Xray Spectrometer (EDS). The upper left hand photograph is a secondary electron image of most of the crater area (left) and some of the unworn tool surface (right). The light triangular band in the middle of the picture is a worn portion of the coating. Xray spectra were taken in

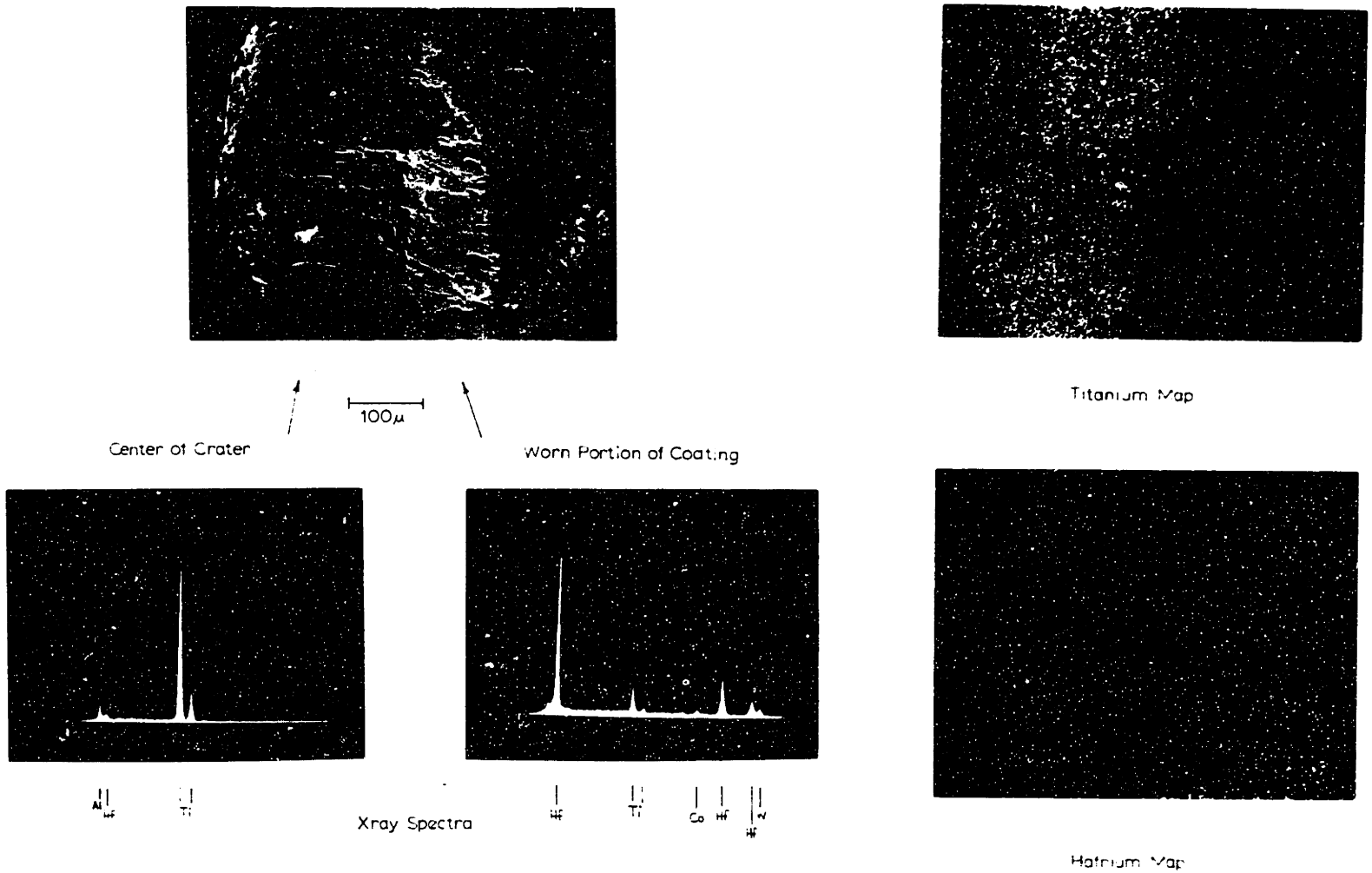

Figure 16. SEM/EDS Analysis of an HfN Coated WC Tool After Turning Ti 6Al-4V

the center of the crater and in the worn portion of the coating. In the center of the crater, the titanium primary and secondary peaks dominate the spectrum, except for a slight amount of hafnium and aluminum (from the alloy). An elemental map of titanium on the surface is obtained by filtering out all energy levels except those associated with the titanium primary peak. As can be seen in the titanium map, titanium covers most of the crater area. Hafnium dominates the spectrum from the worn portion of the coating (triangular region). Carbon and nitrogen are not detected by EDS. A small amount of titanium is also present in this area, along with tungsten and cobalt from the cemented carbide substrate. An elemental map of hafnium shows that the coating is intact on the upper half of the cutting edge, which appears as the smooth area in the secondary electron image. Also, the coating is intact up to the area which is covered by titanium, indicating that the coating wore fairly smoothly, without gross delamination.

Figure 17 shows a polycrystalline diamond tool (Syndite^{R}) which has turned Ti 6Al-4V at 200 sfpm for one minute. The image in the upper left hand corner is a backscatter electron image, which gives more contrast from compositional differences than the secondary electron image (Figure 16). It is clear, from the high magnification photo of the crater area and the titanium map, that a layer of titanium is present

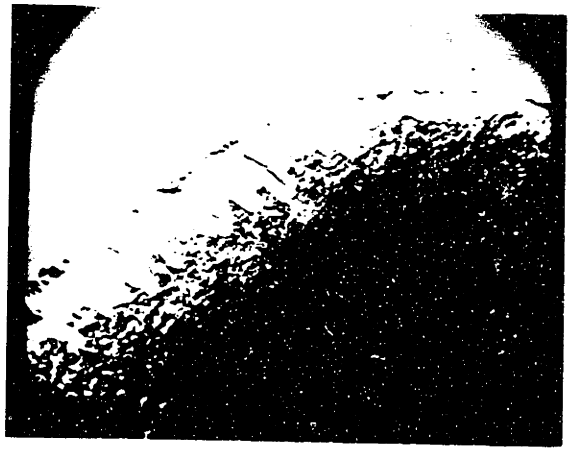

200μ

Titanium Map

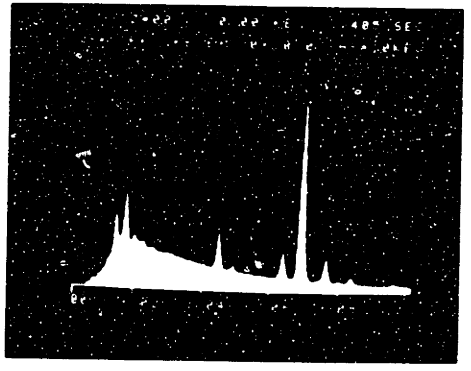

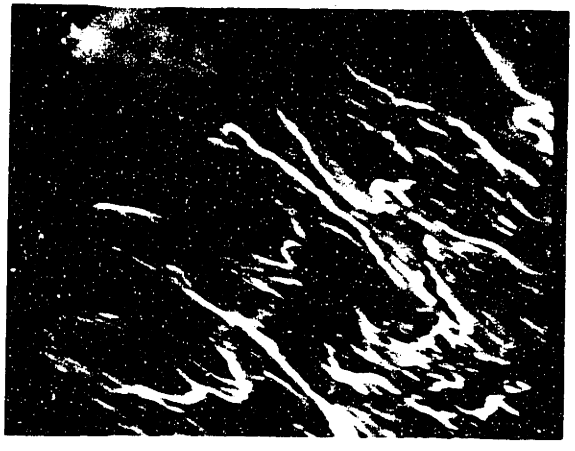

20μ

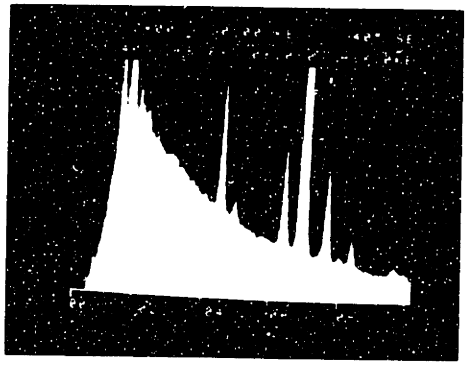

DEBEERS SYNDITE SNG432
CUTTING SPEED: 200 SFPM (61 m/min.)
CUTTING TIME: 1 MIN.
COOLANT: SOLUBLE OIL

Figure 17. SEM/EDS Analysis of a Diamond Tool After Turning Ti 6Al-4V

over the entire crater area, and that over a good portion of that area the layer is very smooth. At this stage, the tool showed essentially no wear. The Xray spectrum of an unworn portion of the tool shows that a fair amount of cobalt is present in the tool material, along with small amounts of tungsten and iron. It is likely that the Co and W diffused through the diamond from the cemented tungsten carbide dies that were employed in the bonding process. The reason for the presence of iron (Fe) is not clear. The trace amounts of molybdenum (Mo) and zirconium (Zr) probably also came from the bonding process.

The same Compax^{R} tool which is shown in the optical micrographs of Figures 10 through 13 is shown before (Figure 18) and after etching in hydrofluoric acid (HF) for 20 minutes (Figure 19). Hydrofuoric acid reacts violently with metallic titanium and slowly with titanium carbide and was, therefore, used to remove any unbound titanium that might be present. Figure 18 shows a backscatter image (top left) of the rake face, and its associated titanium map, as well as a secondary image of both the rake and flank surfaces at the tool tip. The scalloped wear pattern is very clear in these pictures, with the areas of least wear corresponding to the narrower portions of the crater area. Titanium covers the worn areas of the tool. After etching, the tool was analysed on an AMR SEM with a Tracor Northern TN-2000 EDS (Figure 19). Secondary images show the topography of

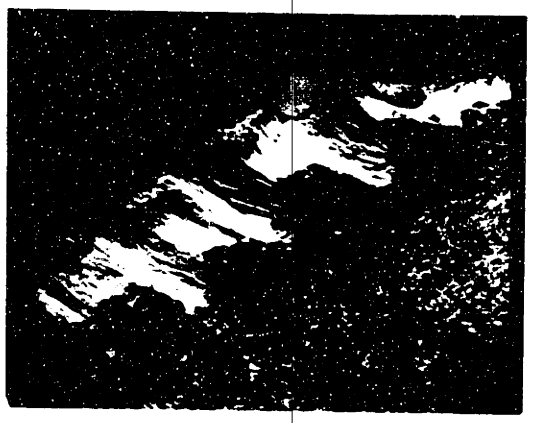

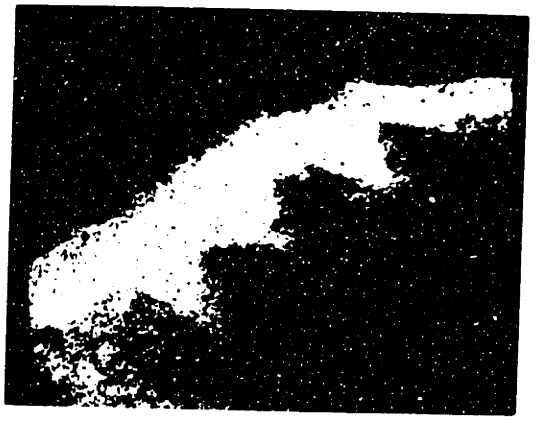

Titanium Map

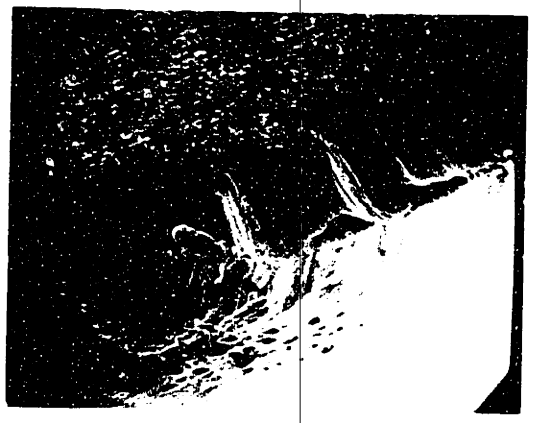

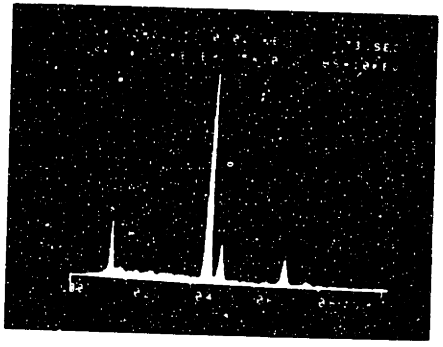

G.E. COMPAX SNG 432
CUTTING SPEED: 200 SFPM (61 m/min.)
CUTTING TIME: 20 MIN.

Figure 18. SEM/EDS Analysis of a Diamond Tool After Turning Ti 6Al-4V

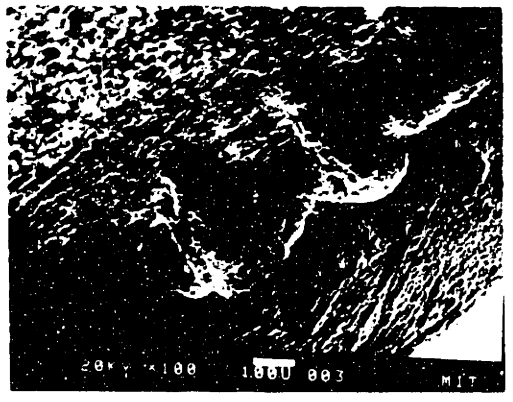

200μ

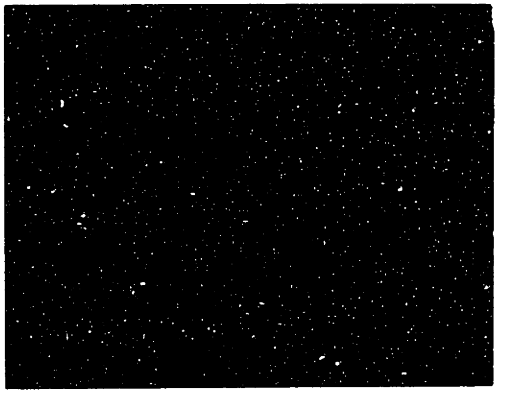

Titanium Map

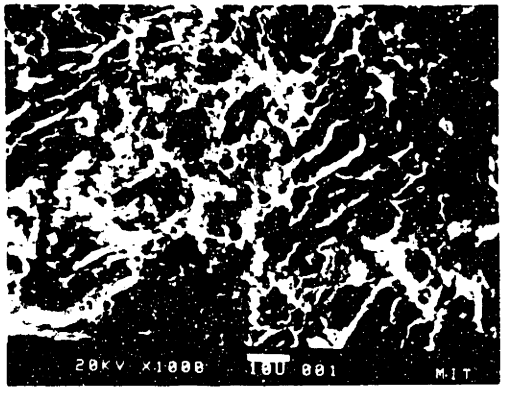

20μ

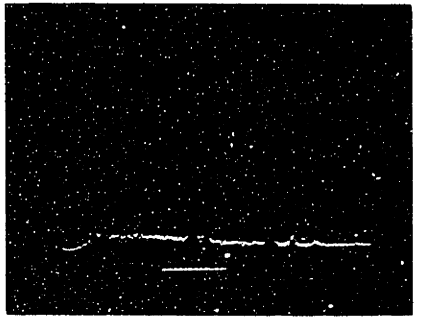

Xray spectrum for magnified portion of crater shown at left

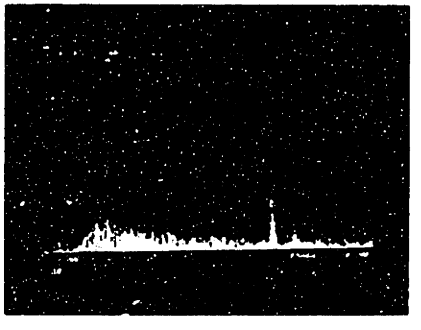

Xray spectrum for unworn portion of top

GE COMPAX SNG 432
(etched in HF for 20 min.)
CUTTING SPEED: 200 SFPM (61 m/min.)
CUTTING TIME: 20 MIN.

Figure 19. SEM/EDS Analysis of a Diamond Tool After Etching

the tool after the unbound titanium has been removed. An Xray spectrum from the crater area shows that titanium is present in some form in the worn portion of the tool after etching, and the elemental map shows the greatest concentration of titanium in the upper right hand corner of the image area, in a region of relatively low wear. Cobalt and tungsten are present in Compax^{R}, as they are in Syndite^{R}, but no iron was detected.

Figure 20 shows the rake face of a Syndite tool after turning Ti 6Al-4V at 500 sfpm (152 m/min) for 1 min. At the higher cutting speed, the polycrystalline diamond tool shows definite scalloping, and titanium covers the entire worn area. In the high magnification photo of an area of very little wear, it seems as though layers of different composition may be present. The limitation of EDS is that it only gives elemental information, and cannot give any information about compositional state.

IX. Auger Electron Spectroscopy for Analysis of Tool Wear

The Auger electron spectroscopy (AES) technique for chemical analysis of surfaces can be used to unambiguously identify the composition of a solid surface [78]. By ionizing the core level of the surface atoms with an electron beam, kinetic energy is given to Auger electrons. This energy is characteristic of the parent atoms, giving rise to peaks in the secondary electron distribution function, the

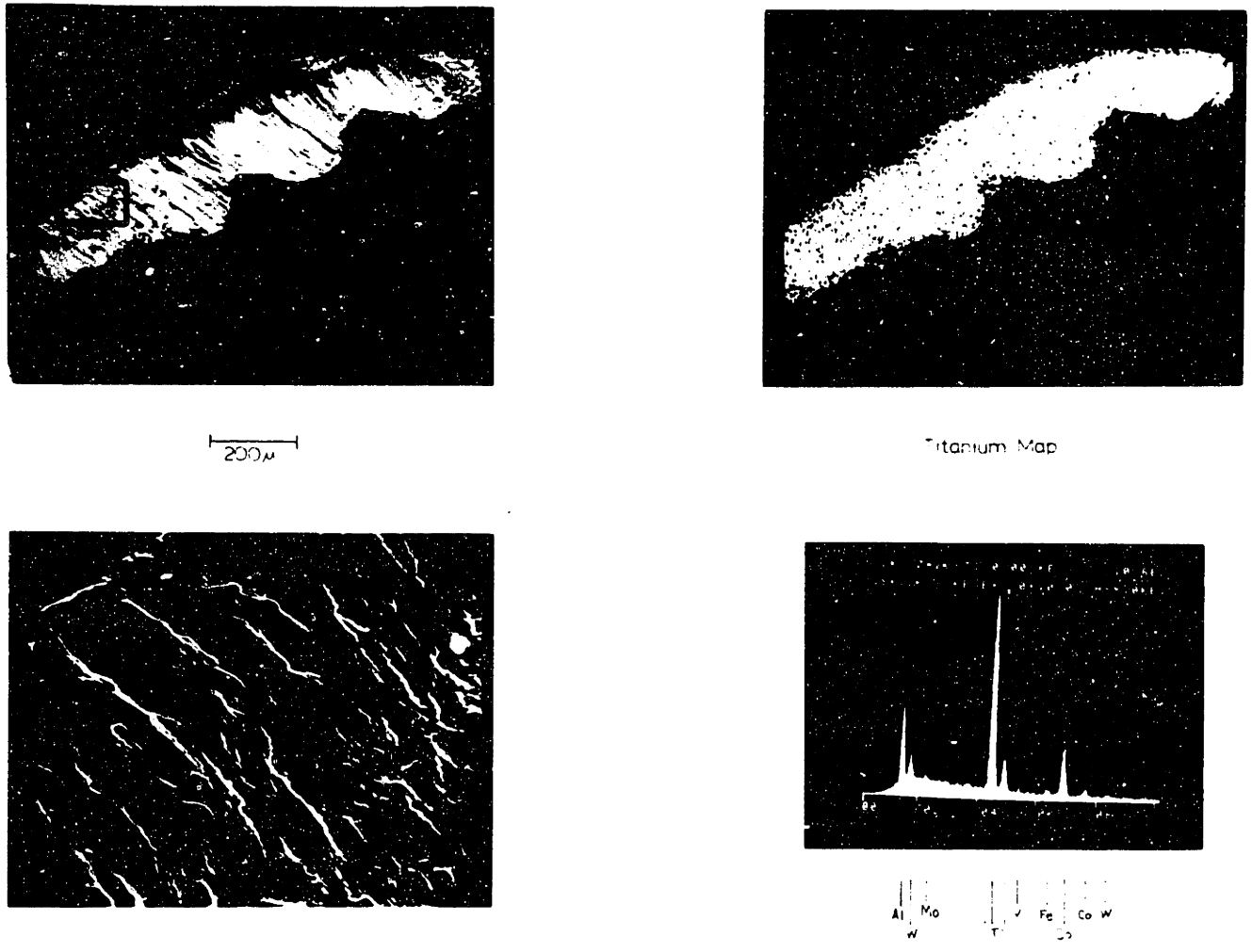

Figure 20. SEM/EDS Analysis of a Diamond Tool After Turning Ti 6Al-4V

energy and shape of which can be used to determine the composition of the surface of the specimen. Quantitative analysis may be accomplished by comparing the peak heights of unknown specimens with those obtained from pure elemental standards or from compounds of known composition. Impurities on the surface of a specimen are removed by sputtering off surface layers with high energy electron beam bombardment within the Auger. Sputtering is also used to determine the change in composition of a specimen with depth below the surface.

To determine whether titanium carbide was formed in the crater area of the diamond tool of Figure 14, Auger spectra were taken of worn and unworn regions of the tool and of a TiC control (an unused Carboloy TiC coated tool). Figure 21 shows Auger spectra from the crater area of the diamond tool after 8, 70, and 130 seconds of sputtering. After 8 seconds of sputtering, peaks corresponding to carbon, titanium and oxygen were present in the crater area of the diamond tool. After 70 seconds of sputtering, the carbon and titanium levels more than doubled, and the oxygen level dropped by about a factor of two. After 130 seconds of sputtering, the titanium and carbon levels dropped slightly, and only a small amount of oxygen is left. Comparison of a spectrum from the crater area of the diamond tool with the spectrum from a TiC control and an unworn portion of the diamond tool reveals a similarity between the carbon emission

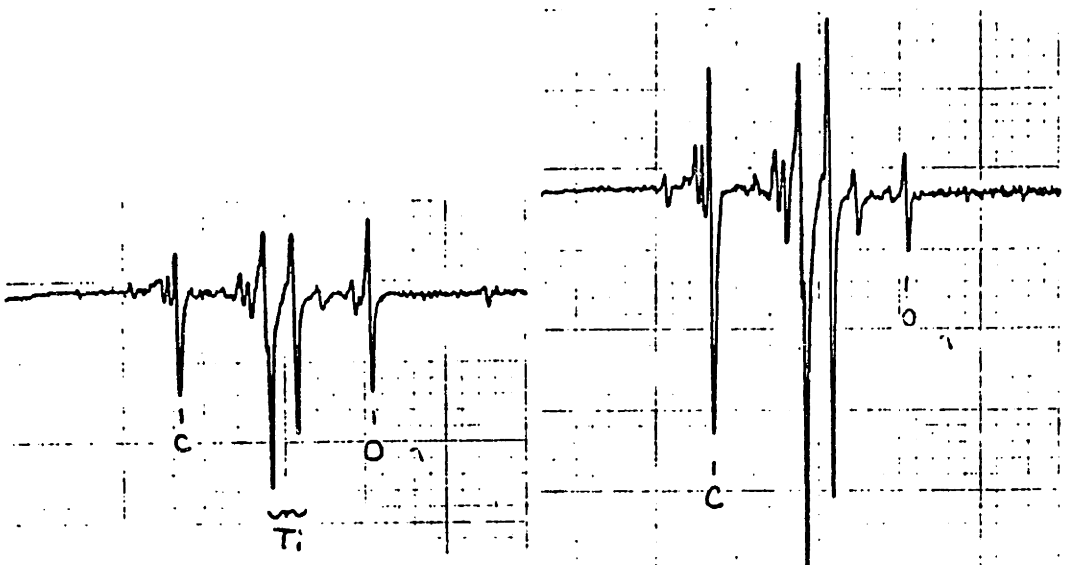

Sputtering Time: 8 seconds

Sputtering Time: 70 seconds

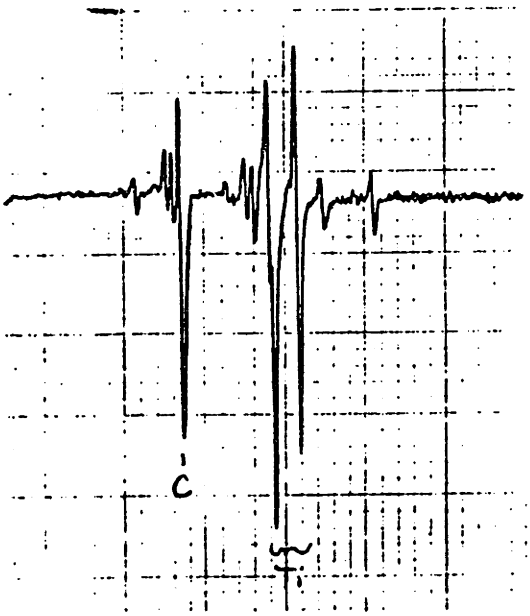

Sputtering Time: 130 seconds

Figure 21. Auger Spectra from the Crater Area of a Diamond Tool which has Machined Ti 6Al-4V

patterns of the crater area and the TiC control which is not characteristic of the unworn diamond material (Figure 22). Analysis of Figures 21 and 22 indicates that titanium oxycarbides are present on the surface of the crater area of the diamond tool, and as the depth below the surface of the tool increases, the oxycarbides decrease in quantity and a layer of relatively pure TiC exists to a depth of on the order of 1000 Angstroms below the surface.

An Auger analysis was performed on a cemented tungsten carbide tool (Kennametal K68, grade C3) which had machined Ti 6Al-4V for 30 seconds (Figure 6). The tool was etched for 20 minutes in HF to remove any pure titanium from the surface before performing the analysis to see if a boundary layer of titanium carbide was formed in the crater area during the cut. An unworn portion of the tool was used as a WC control. Auger spectra taken at three different depths below the crater surface of the tool are shown in Figure 23. After 15 seconds of sputtering, the Auger spectrum shows the presence of tungsten, titanium, bound carbon and oxygen in the crater area of the cemented WC tool. Very little cobalt is present. After 45 seconds of sputtering, the tungsten level increased slightly, the titanium level decreased slightly, and both the carbon and oxygen levels decreased significantly. After a minute more of sputtering, the tungsten level decreased slightly, while both titanium and carbon levels decreased proportionately by about 20%. Oxygen

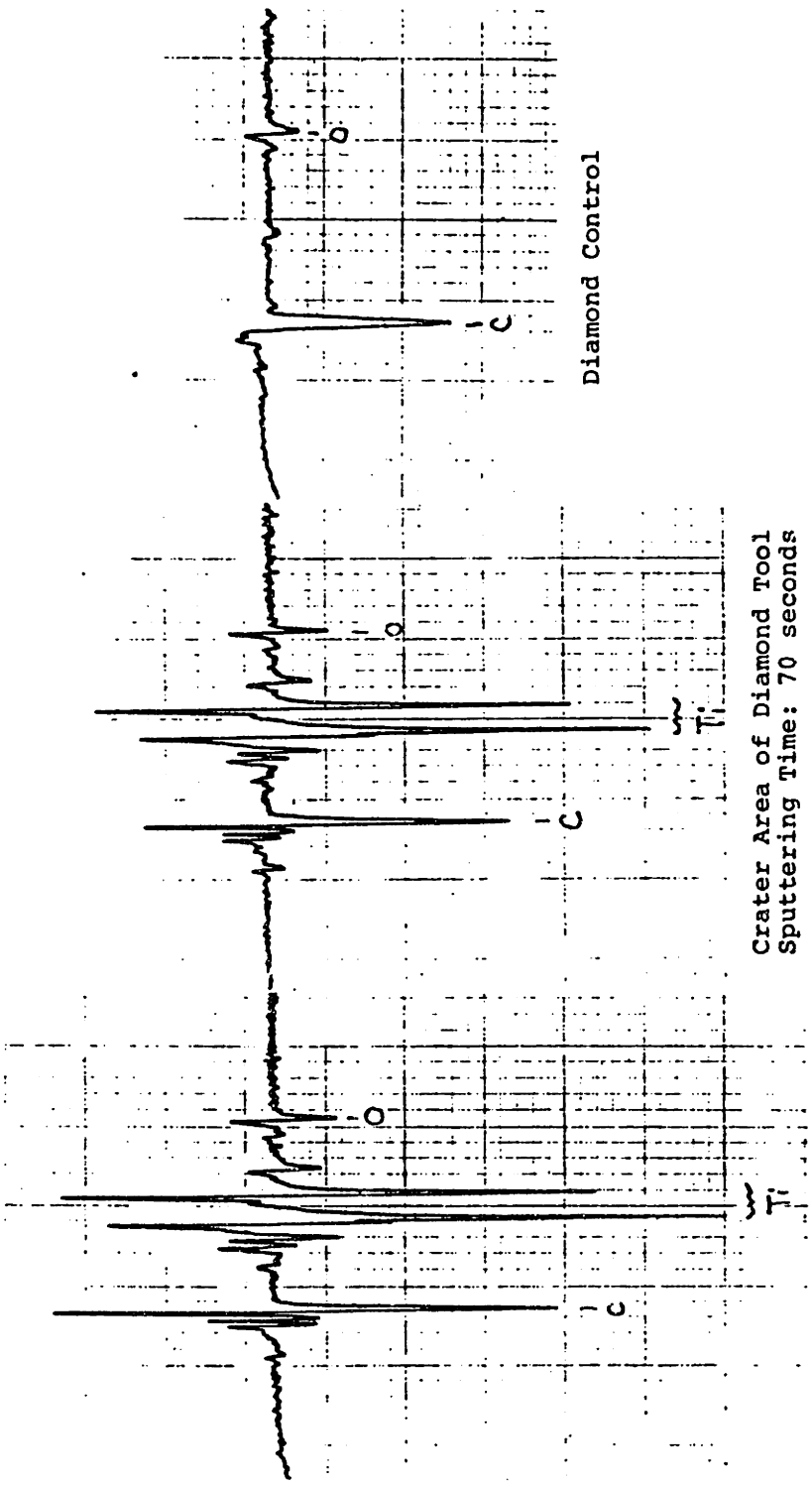

Figure 22. Comparison of an Auger Spectrum from the Crater Area of a Diamond Tool which has Machined Ti 6Al-4V with TiC and Diamond Control Spectra

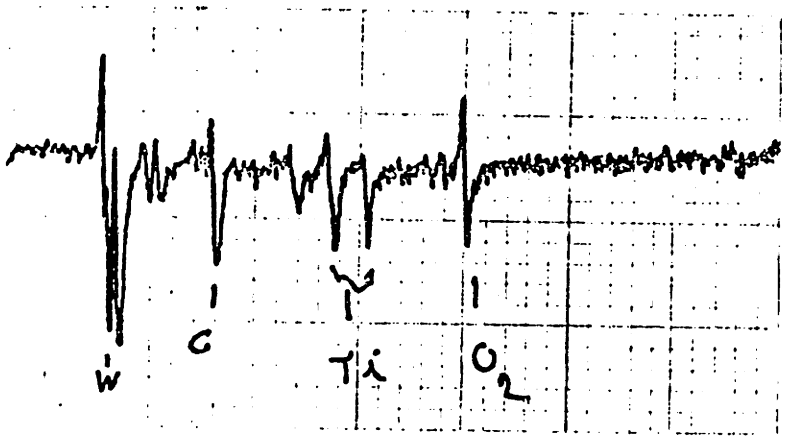

Sputtering Time: 15 seconds

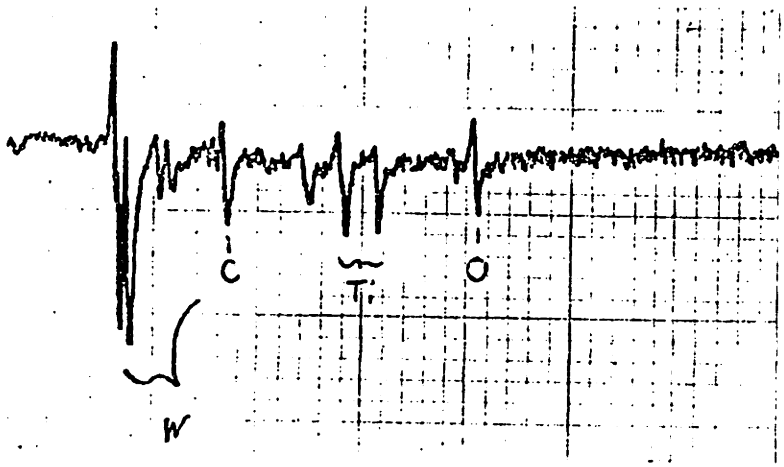

Sputtering Time: 45 seconds

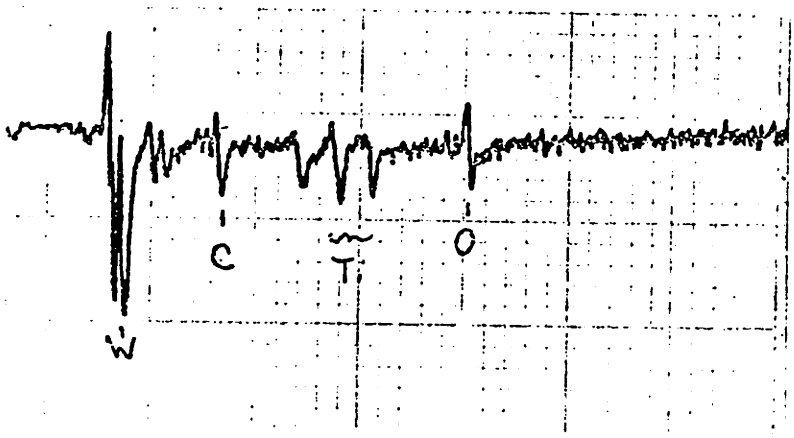

Sputtering Time: 105 seconds

Figure 23. Auger Spectra from the Crater Area of a WC-Based Tool which has Machined Ti 6Al-4V

decreased by less. After 9.75 minutes of sputtering all of the titanium was removed, and the carbon level increased drastically to correspond with the carbon level in the WC control (Figure 24). A measurable amount of cobalt finally appears.

Although the shape of the carbon peak is essentially the same in TiC (Figure 22) and WC (Figure 24), the fact that the carbon level decreases proportionately with the titanium level as the depth below the original crater surface increases, and then increases to correspond with the carbon level of the unworn WC material is a good indication that TiC is forming on the crater surface of the WC-based tools. The presence of oxygen indicates that oxycarbides are also formed during the cut.

The absence of cobalt in the surface layers of the crater of the WC-based tool is an indication that the TiC grains are removed from the surface as a result of binder removal (probably by diffusion), and that the layer of TiC has to be continuously replenished by removing carbon from the WC grains below.

Tests were performed to see if hot-pressed WC with no binder would establish a more stable boundary layer, but the material wore very rapidly due to inadequate bonding between the grains (Figure 25). An Auger analysis was performed

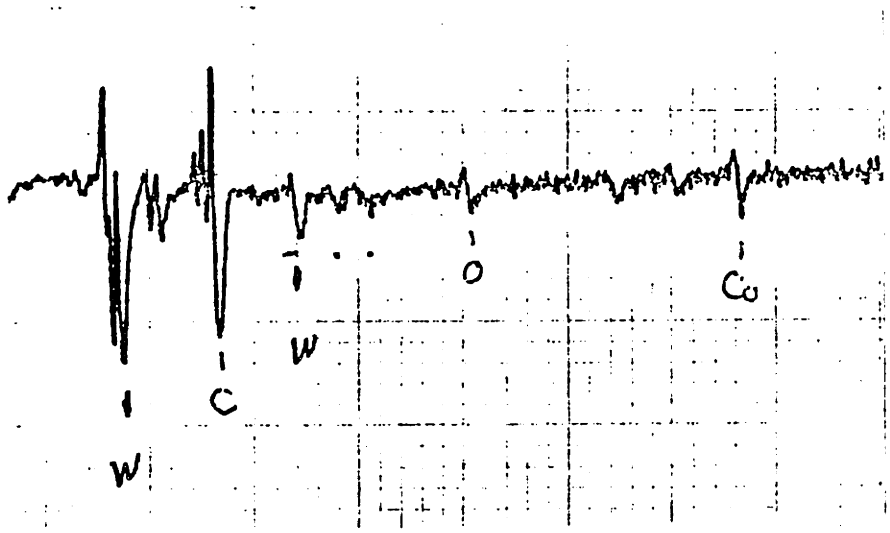

Crater Area of Worn WC-Based Tool
Sputtering Time: 9.75 minutes

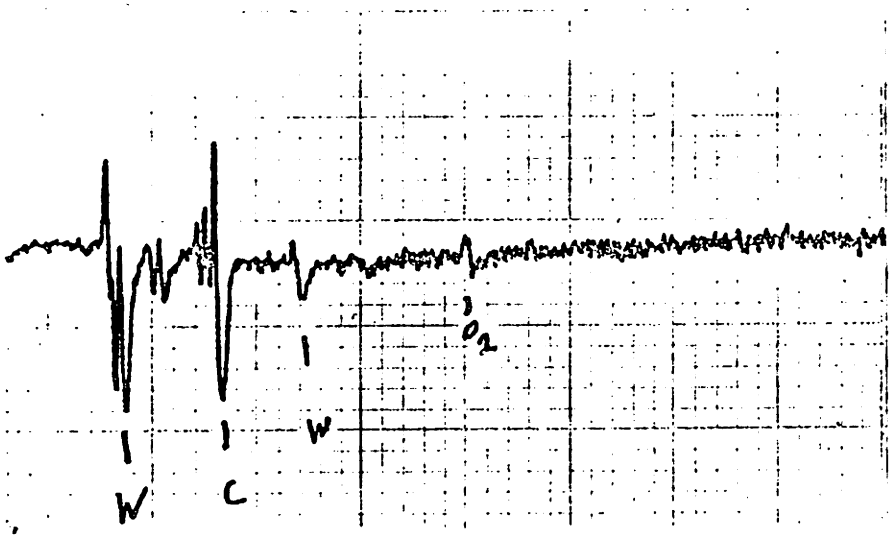

WC Control

Figure 24. Comparison of Auger Spectrum of Sputtered Crater Surface of WC-Based Tool with WC Control Spectrum

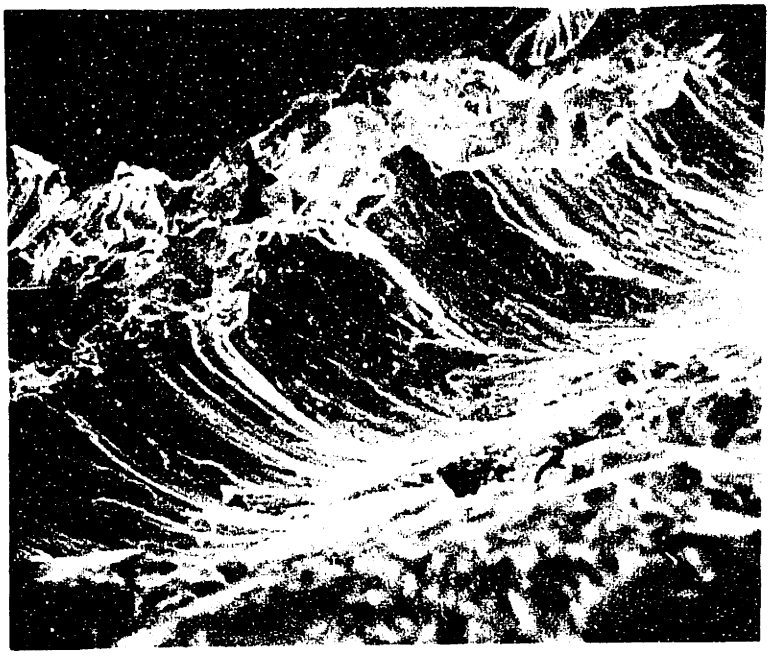

80μ

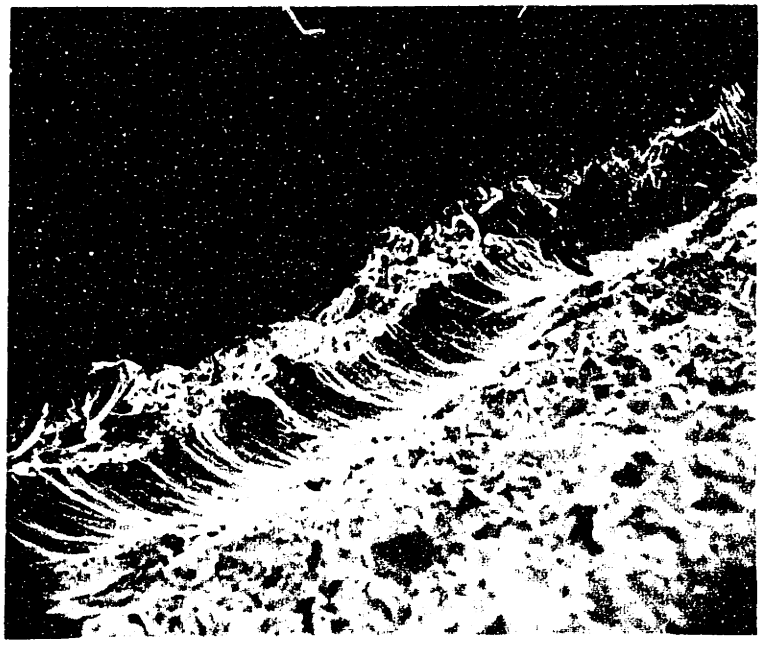

200μ

Figure 25. Micrographs of a Hot-Pressed WC Tool After 5 Seconds of Turning Ti 6Al-4V at 200 sfpm (61.0 m/min) and .0012 ipr (.030 mm/rev)

and titanium was present to a depth of approximately 100 Angstroms, but seemed to be mixed into the surface layers of the tool as opposed to forming a stable layer of its own.

An Auger analysis of cubic boron nitride was performed to see if a stable boundary layer is formed in the areas of low wear on this tool material. Auger spectra of a region of high wear on the Borazon^{R} tool of Figure 6, which has been etched for 20 minutes in HF, show that very little titanium is present in any form in the highly worn region. The titanium was removed in less than one minute of sputtering (Figure 26). The same results were obtained in other locations on the rake face. Apparently no compounds were formed at the tool/chip interface.

X. Theoretical Implications of the Auger Results

The existence of a 1000 Angstrom layer of TiC on the surface of the diamond tool suggests that the wear rate of the tool might be determined by the rate of diffusion of carbon through the TiC layer.

Kroll has found that graphite crucibles are able to withstand the attack of liquid titanium metal by forming a stable layer of titanium carbide on the surface, which prevents direct contact between the melt and the crucible. The dissolution of carbon in the liquid titanium is slow, since it can only occur by diffusion through the carbide layer [79].

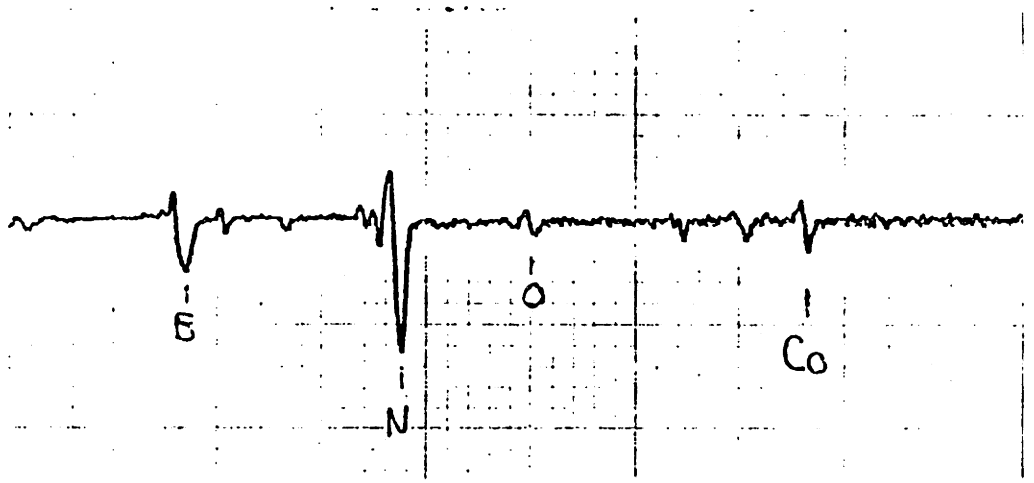

Region of High Wear on CBN Tool
Sputtering Time: 1 minute

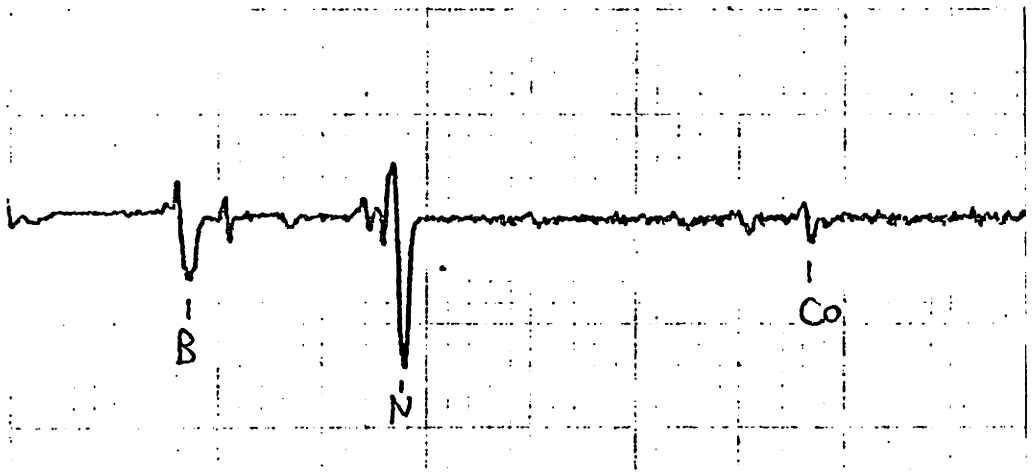

CBN Control

Figure 26. Auger Spectra of Cubic Boron Nitride

Adelsberg and Cadoff [80] have shown that the formation of a TiC layer on graphite from molten titanium follows a parabolic growth law of the form:

$$X^2 = K_p t$$

$$K_p^{TiC} = 0.2 \exp(-61800/RT) \quad cm^2/sec$$

where: X = layer thickness, cm

K_p = parabolic growth constant, cm^2/sec

t = carburization time, sec

T = temperature, °K

In Table 5, the rate of growth of the TiC layer is predicted at 1300, 1400 and 1500°K under the assumption that the parabolic growth law holds at temperatures under the melting point of titanium. As can be seen in the table, it takes less than 0.5 seconds to establish a 1000 Angstrom layer at 1500°K under static conditions.

Table 5 Predicted Growth of a TiC Layer on Diamond

Temperature T°K	Parabolic Growth Constant [80] K_p^{TiC} (cm^2/sec)	Time t(min)	Layer Thickness X(microns)	Time (sec) for layer of thickness 500A	750A	1000A
1300	9.510×10^{-12}	1	0.239	2.629	5.915	10.52
		20	1.068			
1400	5.194×10^{-11}	1	0.558	0.481	1.083	1.925
		20	2.497			
1500	2.262×10^{-10}	1	1.165	0.111	0.249	0.442
		20	5.210			

In Appendix E, a theoretical prediction of the diffusion flux through a 1000 Angstrom layer of TiC is used to predict the wear rate of diamond in titanium. The predicted wear rate (0.10 to 1.8 microns/min at temperatures from 1300 to 1500°K) agrees quite well with the actual wear rate (0.6 to 1.6 microns/min).

If the wear rate of tungsten carbide is also dependent on the diffusion of carbon through a TiC layer, then assuming that the molecular size factor (molar volume of WC/atomic volume of C in diamond = 2.32) is the only added influence on the wear rate, the wear rate of WC is predicted to be from 0.24 to 4.3 microns/min. This also agrees with the wear rate of cemented WC, which is from 2.2 to 2.5 microns/min.

If this model is correct, then the wear rate of tool materials which form a stable layer will be very dependent on the thickness of the layer which is maintained. Also, the presence of a large amount of carbon in the workpiece might reduce the concentration gradient and slow down diffusion.

XI. CONCLUSIONS

Most potential tool materials either rapidly dissolve in or chemically react with titanium when they are used to machine titanium alloys. When chemical reaction occurs, a reaction layer forms, the thickness of which is determined by the balance between the rate of diffusion of tool material through the layer, and the rate of dissolution of the reaction layer in the workpiece. It is suggested that the wear rate of tool materials which maintain a stable reaction layer is limited by the diffusion flux of tool material through the layer.

Calculations based on this diffusion limited model accurately predict the wear rates of polycrystalline diamond and tungsten carbide. These materials showed experimental evidence of the formation of a stable reaction layer, and were the most wear resistant materials tested.

For these materials for which a stable layer forms, it may be possible to reduce tool wear by saturating the titanium workpiece with the fastest diffusing tool constituent, thereby reducing the driving force for diffusion, by effectively eliminating the concentration gradient of the element within the workpiece.

APPENDIX A

Estimation of Solubilities of Potential Tool Materials From Thermochemical Data

For dissociation of the tool material to occur, chemical equilibrium requires that the free energy of formation of the tool material be equal to the sum of the relative partial molor free energies of solution of the tool constituents:

$$\Delta G_{ij} = \Delta \bar{G}_i^m + \Delta \bar{G}_j^m \qquad \text{(A1)}$$

where:

ΔG_{ij} = the free energy of formation of the tool material

$\Delta \bar{G}_i^m$ = the relative partial molar free energy of solution of component i

Assuming that the solution obeys Henry's law, the relative partial molor free energy of solution of component i may be expressed in terms of its relative partial molor excess free energy of solution, $\bar{G}_i^{xs}$, and its equilibrium concentration, C_i, at the temperature of interest, T:

$$\Delta \bar{G}_i^m = \Delta \bar{G}_i^{xs} + RT\ln C_i \qquad \text{(A2)}$$

For a tool material which is a binary alloy with a composition of the form, X_aY_b, Equation A1 may be rewritten as:

$$\Delta G_{tool} = a\Delta\bar{G}_x^m + b\Delta\bar{G}_y^m \qquad (A3)$$

where:

a = number of atoms of component X per molecule of tool material

b = number of atoms of component Y per molecule of tool material

Substituting Equation A2 for both components into Equation (A3) gives:

$$\Delta G_{tool} = a\Delta\bar{G}_x^{xs} + b\Delta\bar{G}_y^{xs} + aRT\ln C_x + bRT\ln C_y \qquad (A4)$$

The concentrations of the tool constituents, C_x and C_y, are equal to the product of the number of atoms of the constituents per molecule of tool material and the equilibrium concentration (solubility) of the tool material, C_{tool}:

$$C_x = a\, C_{tool} \qquad (A5)$$

$$C_y = b\, C_{tool}$$

Substituting in Equation A4 and solving for the solubility of the tool material, the solubility is expressed in terms of the free energy of formation of the tool material and the excess free energies of its constituents in the material being cut. For a tool material of composition X_aY_b:

$$C_{tool} = \exp\left[\frac{\Delta G_{tool} - a\Delta\bar{G}_x^{xs} - b\Delta\bar{G}_y^{xs} - aRT\ln A - bRT\ln b}{(a + b)\ RT}\right] \quad (A6)$$

The free energies of formation of potential tool materials at 1300, 1400, 1500°K, obtained from the literature, are given in Table A1. The solubilities of the tool materials, calculated using Equation A6, are given in Table A2.

The excess free energies of the tool constituents of interest are contained in Tables B1 and B2. The methods used in obtaining the excess free energies are discussed in Appendix B.

In several cases, Equation A6 predicted a solubility of over 100%, which means that chemical reaction would occur, and the solubility measure becomes meaningless.

Table A1 Free Energies of Formation of Tool Materials

	ΔG (cal/mole)			
	1300°K	1400°K	1500°K	Reference
HfC	-49,750	-49,552	-49,354	[81]
NbC	-32,374	-32,338	-32,284	[81]
SiC	-10,600	-10,500	-10,300	[82]
TaC	-34,648	-34,646	-34,612	[81]
TiC	-40,580	-40,240	-39,880	[81]
VC	-23,910	-23,738	-23,602	[81]
ZrC	-43,722	-43,380	-43,034	[81]
BN	-32,700	-30,500	-28,300	[82]
HfN	-59,084	-56,916	-54,756	[83]
Si_3N_4	-75,161	-67,354	-59,583	[84]
TiN	-51,560	-49,698	-47,298	[81]
Al_2O_3	-301,700	-293,900	-286,100	[82]
HfO_2	-206,000	-202,000	-196,600	[85]
La_2O_3	-312,000	-307,500	-303,000	[85]
ZrO_2	-204,000	-199,000	-194,200	[85]
TiB_2	-68,397	-68,066	-67,735	[86]

Table A2 Estimated Solubilities of Tool Materials in Titanium

Tool Material	Solubility, C (mol. %) 1300°K	1400°K	1500°K
HfC	1.27	1.41	1.53
NbC	23.70	20.73	18.45
SiC	*	*	*
TaC	16.03	14.32	13.02
TiC	7.75	7.75	7.75
VC	*	*	*
WC	*	*	*
ZrC	4.23	4.42	4.58
BN	*	*	*
HfN	10.92	12.80	13.35
Si_3N_4	*	*	*
TiN	48.58	48.48	48.17
Al_2O_3	*	*	*
HfO_2	7.85	14.67	29.46
ZrO_2	10.47	21.58	39.50
La_2O_3	0.033	0.076	0.155
TiB_2	*	*	*

*Chemical reaction occurs.

Appendix B Estimation of the Excess Free Energies of Solution of Tool Constituents in Titanium

Although reasonably reliable free energy of formation data is available for most potential tool materials, the excess free energies of solution of most tool constituent materials in titanium have not been measured. Miedema et.al [87] have demonstrated that the heat of formation of binary intermetallic compounds that contain at least one transition metal and that of liquid alloys in general can be described in terms of a simple atomic model, and have predicted the heats of solution of many liquid metals in liquid metal solvents. The heat of solution is simply the excess free energy of solution at the melting point of the metals, and assuming that the excess free energies are relatively temperature independent, have been taken as a measure of the excess free energies of solution of metal tool constituents in titanium at the cutting temperature. Table B1 lists the estimated excess free energies of solution of metal tool constituents in titanium, along with their melting points. The excess free energies of solution of boron, carbon, nitrogen and oxygen are found by solving for $\Delta\bar{G}_i^{xs}$ in Equation A2:

$$\Delta\bar{G}_i^{xs} = \Delta\bar{G}_i^{m} - RT\ln C_i \qquad (B1)$$

Table B1 Melting Points and Estimated Excess Free Energies of Solution of Tool Constituents in Titanium

Solute i	Melting Point°K [71]	$\Delta\bar{G}_i^{xs}$ (cal/mole) [87]
Al	933.52	-32744
Hf	2500±20	239.0
La	1194	32505
Nb	2741±10	2390
Si	1683	-50430
Ta	3269	2151
Ti	1933±10	0
V	2163±10	-1912
W	3683±20	-6214
Zr	2125±2	0

Kubaschewski [88] has plotted the free energy of dissociation of oxygen in titanium for the full range of concentrations of oxygen at 1273°K and 1473°K. Using Equation A7, the excess free energy of solution of oxygen in titanium was calculated to be -95,000 ± 8500 cal/mole in that temperature range. Since solubilities were to be estimated at 1300°K, 1400°K and 1500°K, $\Delta\bar{G}_o^{xs}$ was taken to be -95,000 cal/mole.

The free energies of solution of B, C and N per mole of the respective atoms at the solubility limits must be equal to the free energies of formation of TiB, TiC and TiN, the phases with which the saturated solutions are in chemical

equilibrium. The solubility limits and nature of the second phases are obtained from phase diagrams.

The free energy of formation of TiB was not available so it was estimated from the free energy of formation of TiB_2, assuming that the free energies of formation are equal on a gram-atom basis.

The excess free energies of solution of B, C, and N estimated at 1300°K, 1400°K and 1500°K are given in Table B2 along with their free energies of solution and solubility limits.

Table B2 Excess Free Energies of Solution of Boron, Carbon and Nitrogen in Titanium

Tool Constituent, i	T(°K)	Solubility Limit C_i (at %)		Free Energy of Solution $\bar{\Delta G}_i^m$ (cal/mole)	Excess Free Energy of Solution $\bar{\Delta G}_i^{xs}$ (cal/mole)
B	1300	1.	[67]	-68,397	-56,424
	1400	1.	"	-68,066	-55,172
	1500	1.	"	-67,735	-53,919
C	1300	0.6	[68]	-40,580	-27,278
	1400	0.6	"	-40,240	-25,915
	1500	0.6	"	-39,880	-24,532
N	1300	23.6	[68]	-51,560	-47,806
	1400	23.5	"	-49,698	-45,643
	1500	23.2	"	-47,298	-42,915

Appendix C Tool Wear Prediction Based on Laminar Boundary Layer Theory

Since there is evidence that no relative sliding occurs under certain conditions at the tool/chip interface, it was thought that an upper bound for the wear rate might be obtained by treating the chip as a flow of "liquid" titanium over the tool and using the solution for mass transfer in the laminar boundary layer on a flat plate.

The solution, which is described in detail by Skelland [80], assumes that the relative velocity at the interface is zero and that the fluid is Newtonian (viscosity is constant). Defining the momentum boundary layer thickness, δ, as the distance from the surface where the flow velocity reaches 0.99V, where V is free stream chip velocity and assuming a cubic polynomial form for the velocity distribution, the solution is given as:

$$\frac{\delta}{X} = 4.64 \left(\frac{\mu}{\rho V X}\right)^{\frac{1}{2}} = 4.64\ N_{Re}^{-\frac{1}{2}} \qquad \text{(C1)}$$

where:
- δ = momentum boundary layer thickness
- X = distance from edge of tool
- μ = viscosity of the metal
- ρ = density of the metal
- V = free stream chip velocity
- $N_{Re} = \frac{\rho V X}{\mu}$ (Reynold's number)

The concentration boundary layer thickness, δ_c, is

defined as the distance from the surface of the tool

where: $$C_{Ao} - C_A = 0.99\ (C_{Ao} - C_{Aoo}) \qquad (C2)$$

where: C_A = mass concentration of the diffusing component A

C_{Ao} = mass concentration of A at the tool surface

C_{Aoo} = mass concentration of A in free stream

Assuming a cubic polynomial form for the concentration distribution, the approximate solution for δ_c is given as:

$$\frac{\delta_c}{\delta} = 0.976\ N_{Sc}^{-\frac{1}{3}} \left[1 - \left(\frac{Xo}{X}\right)^{\frac{3}{4}}\right]^{\frac{1}{3}} \qquad (C3)$$

where: δ_c = concentration boundary layer thickness

X_o = distance from leading edge where mass transfer begins

$N_{Sc} = \frac{\mu}{\rho D}$ (Schmidt number)

D = diffusion coefficient of component A in the chip

Assuming that mass transfer begins at the leading edge of the plate ($X_o = 0$), Equation (C3) simplifies to:

$$\delta_c = \delta N_{Sc}^{-\frac{1}{3}} \qquad (C4)$$

Substituting for δ from Equation (C1), gives:

$$\frac{\delta_c}{x} = 4.64\ N_{Re}^{-\frac{1}{2}}\ N_{Sc}^{-\frac{1}{3}} \qquad (C5)$$

The mass flux from the tool surface, n_{Ao}, can be expressed in terms of a local mass transfer coefficient, K, at the surface:

$$n_{Ao} = -K(C_{Aoo}-C_{Ao}) \tag{C6}$$

An expression for K is obtained directly from the mass flux equation and the definition of the mass boundary layer thickness, Equation (C2):

$$-K = \frac{n_{Ao}}{C_{Aoo} - C_{Ao}} = \frac{-D}{C_{Aoo} - C_{Ao}} \frac{\partial (C_A - C_{Ao})}{\partial y} \tag{C7}$$

$$= \frac{-3}{2} \frac{D(C_{Aoo} - C_{Ao})}{(C_{Aoo} - C_{Ao})\ \delta_c} = \frac{-3}{2} \frac{D}{\delta_c}$$

Inserting Equation (C5) for δ_c, the local mass transfer coefficient at the tool surface is given by:

$$K = \frac{0.323\ N_{Re}^{\frac{1}{2}}\ N_{Sc}^{\frac{1}{3}} D}{x} \tag{C8}$$

In the limiting case where the chip is assumed to be a flow of liquid titanium over the tool surface, the momentum and mass diffusion boundary layer thickness and the mass transfer rate from the tool surface at the center of the crater can be calculated from the flow velocity, which is

assumed to be the chip velocity, the density and viscosity of liquid titanium, the diffusion coefficient of the tool material in the chip, and the distance from the edge to the center of the crater.

The viscosity of liquid titanium is approximately .001 Pa-s and the density of titanium is approximately 4.35 g/cm^3 [79]. If we assume that the other parameters are the same as used in the upper bound diffusion flux prediction (Section VII.E) the predicted boundary layer thicknesses and mass transfer rate are as given in Table C1. It is quite clear that this solution is an upper bound, and predicts a much higher wear rate than actually exists.

Table C1 Predicted Boundary Layer Thicknesses and Mass Transfer Rate For Liquid Titanium Flowing Over a Diamond Tool Surface

Cutting Speed (m/min)	Boundary Layer Thickness		Mass Transfer Coefficient K(m/sec)	Predicted Wear Rate (microns/min)
	Momentum δ (m)	Concentration δ_c (m)		
61.0	1.25×10^{-5}	1.25×10^{-6}	2.75×10^{-4}	1.65×10^{4}

Appendix D Model Prediction for the Wear of Diamond In the Machining of Titanium

Since the existence of a reaction layer of TiC has been established on the surface of diamond tools which have been used to machine titanium, it may be possible to model the wear process as a diffusional process where the driving force is the concentration gradient of carbon across the reaction layer.

In Figure D1, a simple model for the wear process is shown, where the wear rate is given by:

$$V_{wear} = -MD \frac{\partial c}{\partial y} = -MD \frac{C_B - C_s}{t} \qquad (D1)$$

where: V_{wear} = the wear rate of the tool (cm/sec)

M = molar volume of tool material (cm^3/mole)

D = diffusion coefficient of carbon through the reaction layer (cm^2/sec)

C_B = concentration of carbon at the reaction layer/chip boundary

C_o = concentration of carbon at the tool surface/reaction layer boundary

t = thickness of the reaction layer

There is a large amount of variation in reported diffusion coefficients for carbon in TiC, as is shown in Table D1. The values at the top of the table were considered the most reliable and were used in predicting the wear rate. The

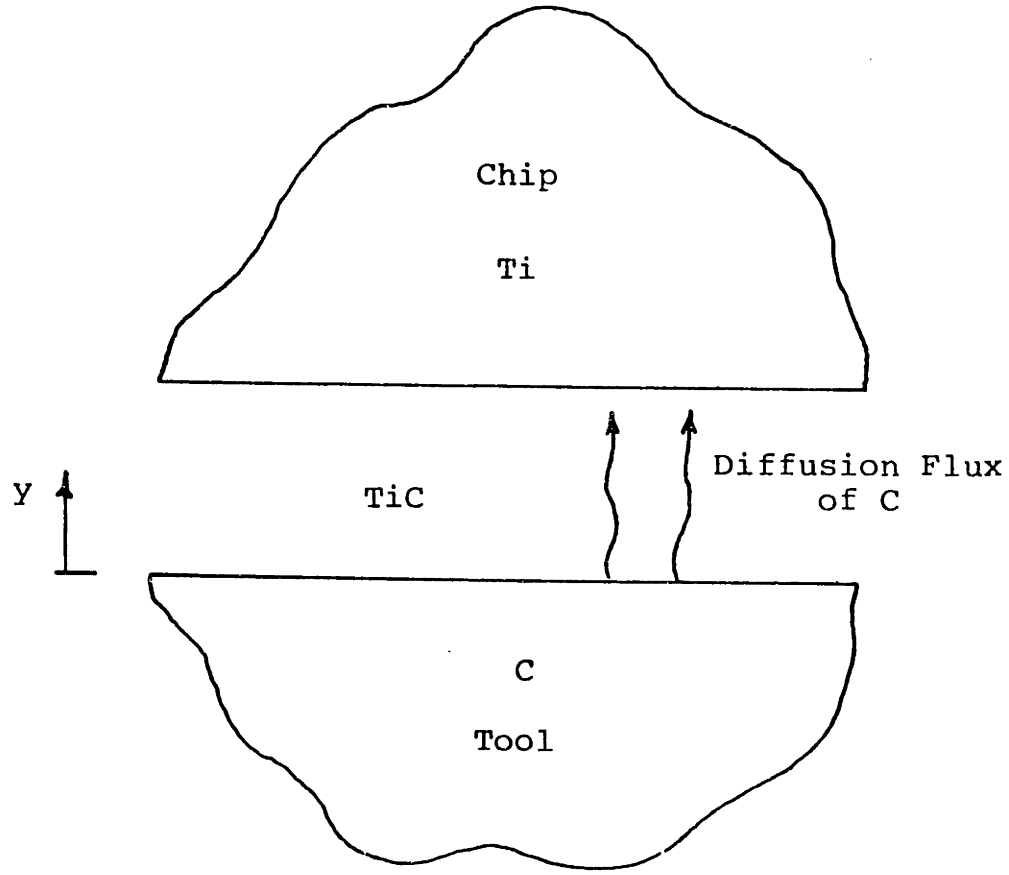

Figure D1. Model for the Wear of Diamond by Diffusion Through a Reaction Layer of TiC.

Table D1 Diffusion Coefficients for C in TiC

Ref.	Composition	Solute	Technique	D_o cm^2/sec	Q kcal/mole	D cm^2/sec at 1300_k	1400_k	1500_k
[80]	TiC	C	layer growth (1800-2700°C)	.05	56300 (R=2)	1.97×10^{-11}	9.26×10^{-11}	3.54×10^{-10}
[90]	$TiC_{0.970}$	C^{14}	serial sectioning (1450-2280°C)	6.98 ± 1.24	95.3 ± 0.7	6.65×10^{-16}	9.27×10^{-15}	1.12×10^{-13}
[90]	$TiC_{0.887}$	C^{14}	same	45.44 ± 5.12	106.8 ± 0.4	5.05×10^{-17}	1.24×10^{-15}	1.57×10^{-14}

reaction layer thickness, t, was assumed to be 1000 Angstroms, which was the approximate measured value in the AES study.

In Table D2 the method of calculating the wear rate from phase diagram data for the concentrations at the boundaries is outlined. The predicted wear rate of diamond correlates well with the observed wear rate.

The wear rate of WC is also calculated assuming that the diffusion of carbon controls the wear. The molar volume of WC is assumed to be the only added factor in determining the wear rate.

Table D2 Prediction of the Wear Rates of Diamond and WC By Diffusion Through a Layer of TiC

Parameter	Reference	Ti/TiC Boundary Temperature 1300°K	1400°K	1500°K	C/TiC Boundary All 3 Temp's.
C_c (at %)	[66]	33.0	33.5	34.0	49.0
latt. par., a (Å)	[67]	4.304	4.306	4.308	4.328
unit cell volume ($Å^3$)		79.73	79.84	79.95	81.07
mol. vol. TiC ($Å^3$)		19.93	19.96	19.99	20.27
mol. vol. TiC/atom C ($Å^3$/atom)		30.20	29.79	29.39	20.68
mol. vol. (cm^3/mol C)		18.19	17.94	18.24	12.45
conc. of C in TiC (mole/cm^3)		5.498×10^{-2}	5.574×10^{-2}	5.483×10^{-2}	8.029×10^{-2}
Diffusion Flux, J (moles/cm^2-sec)		4.986×10^{-8}	2.274×10^{-7}	9.013×10^{-7}	
V_{wear} (Diamond) (cm/sec)		1.705×10^{-7}	7.775×10^{-7}	3.082×10^{-6}	
V_{wear} (Diamond) (μ/min)		0.102	0.467	1.849	
V_{wear} (WC) (μ/min)		0.237	1.084	4.294	

References

[1] "Machinability of Titanium 150 A," American Machinist, October 1, 1951, p. 179.

[2] M. C. Shaw et al., "Machining Titanium," A Report Prepared for the United States Air Force Wright-Patterson Air Force Base, Dayton, Ohio, Under Contract No. AF33 (600) - 22674, M.I.T., Cambridge, Massachusetts, June 1954.

[3] M. C. Shaw, P. A. Smith, B. Colding, N. H. Cook, "Machining Titanium II," A Report Prepared for the United States Air Force Base, Dayton, Ohio, Under Contract No. AF 33 (600) - 31636, M.I.T., Cambridge, Massachusetts, February 1957.

[4] H. J. Siekmann, "How to Machine Titanium," The Tool Engineer, January 1955, pp. 78 - 82.

[5] K. Loo, "North American Research on Machining Titanium Alloys," Machinery, October 1957, pp. 157 - 161.

[6] "Milling Titanium Alloys: Some Practical Results From A Basic Study," Mechanical World, July 1958, pp. 302-304.

[7] L. V. Colwell and L. J. Quackenbush, "A Study of High-Speed Milling of Titanium Alloys," ORA Project 04393, SP-316, University of Michigan, Ann Arbor, October 1961.

[8] L. V. Colwell and L. J. Quackenbush, "A Study of High-Speed Milling, Final Report. Part I. The Role of Shock Waves and Vibrations," ORA Project 05038, University of Michigan, Ann Arbor, September 1962.

[9] L. V. Colwell and L. J. Quackenbush, "A Study of High-Speed Milling, Final Report. Part II. The High-Speed Milling of Titanium Alloys," ORA Project 05038, SP-472, University of Michigan, Ann Arbor, December 1962.

[10] Machining Difficult Alloys, A Compendium on the Machining of High-Strength Steels and Heat Resistant Alloys, sponsored by the United States Air Force, American Society for Metals, Metals Park, Ohio, 1962, pp. 77 - 79.

[11] H. Olynik, "Face Milling and End Milling of Titanium Alloys 6Al-4V and 13V-11 Cr-3Al," GAEC ADR-08-08-64.2, September 1964.

[12] M. Field, N. Zlatin and R. T. Jameson, "Machining Difficult Materials...Titanium Alloys," Metal Progress, February 1965, pp. 84 - 89.

[13] E. Hill and W. J. Maxson, "How Boeing Machines Titanium Aircraft Parts," Metal Progress, February 1965, pp. 90 - 92.

[14] C. A. Brophy, "Machining of Titanium Alloys," DMIC Memorandum 199, Battelle Memorial Institute, Columbus 1, Ohio, February 2, 1965.

[15] R. L. Vaughn, "Modern Metals Machining Technology," Trans. ASME, Journal of Engineering for Industry, February 1966, pp. 65 - 71.

[16] H. C. Child and A. L. Dalton, "Machining of Titanium Alloys, Part 1. Metallurgical Factors Affecting Machinability," Machinability, Proc. of the Conference on Machinability, October 4 - 6, 1965, ISI Special Report 94, Portsmouth, England, 1967, pp. 139 - 142.

[17] E. J. Catt and D. Milwain, "Machining of Titanium Alloys, Part 2. General Machining Behavior of Titanium," Machinability, Proc. of the Conference on Machinability, October 4 - 6, 1965, ISI Special Report 94, Portsmouth, England, 1967, pp. 143 - 150.

[18] J. Maranchik, Jr. and R. E. Snider, "Machining of Titanium Alloys," ASTME Technical Paper No. MR68-801.

[19] F. LeMaitre, "Contribution a l'Usinage du Titane et de ses Alliages," Annals of the C.I.R.P., Vol. XVIII, Great Britain, 1970, pp. 413 - 424.

[20] W. Kreis, "Zerspanbarkeit der Titanwerkstoffe," Industrie-Anzeiger 96. Jg. Nr. 55 V. 3.7. 1974.

[21] R. Komaduri, "Some Clarifications of the Mechanics of Chip Formation When Machining Titanium Alloys," Advanced Machining Research Program (AMRP), General Electric Company Annual Technical Report SRD-80-118, AFWAL/MLTM, August 16, 1980, pp. 5 - 1, 5 - 20.

[22] R. Komanduri, "Further Work on Chip Formation Characteristics when Machining Titanium Alloys," Ibid., pp. 6 - 1 to 6 - 24.

[23] M. Lee, "Innovative Tool Evaluation," Ibid., pp. 8 - 1 to 8 - 3.

[24] M. G. Jones, "Pulse Laser Experiments," Ibid., pp. 19 - 1 to 19 - 15.

[25] T. A. Schroeder and J. Hazra, "Conventional To High Speed Turning of Some Aircraft Alloys," Ibid., pp. 11 - 1 to 11 - 47.

[26] F. W. Gorsler, "Current Limits Turning Aircraft Engine Materials," Ibid., pp. 14 - 1 to 14 - 14.

[27] N. H. Cook, E. Rabinowicz and R. L. Vaughn, "Metal Cutting Lubrication Through Continuous Electroplating," Lubrication Engineering, November, 1966, pp. 447 - 452.

[28] R. L. Vaughn, Private Communication, 8/14/80.

[29] K. Uehara, K. Dambara and Y. Kanda, "An Attempt to Improve the Cutting Performance Through Metallizing," Annals of the C.I.R.P., Vol. XVIV, 1971, pp. 439 - 444.

[30] K. Uehara et al., "Effect of Solid Lubricants in High Speed Intermittent Metal Cutting," Proceedings of the International Conference on Production Engineering (Part 1), JSPE/CIRP, Tokyo, 1974, pp. 566-571.

[31] A. J. Koury, M. K. Gabel, A. P. Wijenayake, "Effect of Solid Film Lubricants on Tool Life," ASLE Reprint No. 78-Am-6E-2, 1978.

[32] R. L. Vaughn, "Ultra-High Speed Machining (Feasibility Study), Phase I," AMC Technical Report 60-7-635(1), June, 1960.

[33] R. F. Recht, "Catastrophic Thermoplastic Shear," Trans. of the ASME, Journal of Applied Mechanics, June, 1964, pp. 189 - 193.

[34] K. Okushima, K. Hitomi, S. Ito and N. Narutaki, "Fundamental Study of Super-High Speed Machining," Bulletin of JSME, Vol. 8, No. 32, 1965, pp. 702 - 710.

[35] Y. Tanaka, H. Tsuwa, M. Kitano, "Cutting Mechanism in Ultra-High-Speed Machining," ASME, 67-Prod-14, 1967.

[36] R. Geslot, J. Girard, R. Weill, "Effort De Coupe En Tournage Pour Des Vitesses De Coupe Allant Jusqu'a 3600 m/min," Annals of the C.I.R.P., Vol. 22/1, 1973.

[37] J. F. Kahles, M. Field and S. M. Harvey, "High Speed Machining Possibilities and Needs," Annals of the C.I.R.P., Vol. 27/2, 1978, pp. 551 - 560.

[38] R. G. Fenton and P. L. B. Oxley, "Predicting Cutting Forces at Super High Cutting Speeds From Work Material Properties and Cutting Conditions," Advances in Machine Tool Design and Research 1967, Proceedings of the 8th International M.T.D.R. Conference, September 1967, pp. 247 - 258.

[39] G. Arndt, "Ultra-High-Speed Machining," Annals of the C.I.R.P., Vol. 21/1, 1972, pp. 3 - 4.

[40] G. Arndt, "Ultra-High-Speed Machining: A Review and an Analysis of Cutting Forces," Proc. Instn. Mechn. Engrs., Vol. 187, 44/73, 1973, pp. 625 - 634.

[41] G. Arndt, "The Development of Higher Machining Speeds - Part 2," The Production Engineer, December 1970, pp. 517 - 529.

[42] G. Arndt and R. H. Brown, "Design and Preliminary Results From An Experimental Machine Tool Cutting Metals At Up To 8,000 Feet Per Second," Proceedings of the Thirteenth International Machine Tool Design and Research Conference, Birmingham, September 18 - 22, 1972, pp. 217 - 223.

[43] R. I. King and J. G. McDonald, "Project Design Implications of New High-Speed Milling Techniques," Trans. ASME, J. Eng. for Industry, November 1976, pp. 1170 - 1175.

[44] M. Lee, "Gas Gun Machining Experiments," Advanced Machining Research Program (AMRP), General Electric Company Annual Technical Report SRD-80-118, AFWAL/MLTM, August 16, 1980, pp. 7 - 1, 7 - 11.

[45] J. P. Kottenstette and R. F. Recht, "An Ultra-High-Speed Machining Facility," Advanced Machining Research Program (AMRP) General Electric Company Annual Technical Report SRD-80-118, AFWAL/MLTM, August 16, 1980, pp. 9 - 1, 9 - 26.

[46] R. J. Delaney, "Sub-Zero Machining and Quenching," Machinery, Vol. 63, No. 11, July, 1957, pp. 148 - 153.

[47] P. W. Wilson and R. W. Cox, Machining the Space-Age Metals, American Society of Tool and Manufacturing Engineers, Dearborn, Michigan, 1965, pp. 98 - 99.

[48] "Cryogenic Coolants Speed Titanium Machining," Machinery, July, 1965, pp. 98 - 99.

[49] D. Koenig, Private Communication.

[50] R. V. Joshi, Mechanical Engineering Thesis, M.I.T., June, 1981.

[51] I. A. Dickter, C. L. Mehl and R. F. Henke, "Final Report on High Temperature Machining Methods," Technical Documentary Report Nr. ASD-TDR-63-125, Wright-Patterson Air Force Base, Ohio, 1963, pp. 219 - 276.

[52] R. H. Wentorf, Jr., "Borazon and Diamond Compacts," Advances in Hard Material Tool Technology, Proceedings of the 1976 International Conference on Hard Material Tool Technology, Carnegie-Mellon University, Pittsburgh, Pennsylvania, June 22 - 24, Carnegie Press, 1976, pp. 510 - 524.

[53] M. D. Dennis and J. D. Christopher, "The Characterization and Performance of Compax Diamond Tools in Machining Applications," SME Technical Paper. No. MR-75-986, 1975.

[54] E. W. Krumrei, "Diamond Tooling Cuts Into Traditional Carbide Uses," Tooling and Production, February 1980, pp. 68 - 71.

[55] G. F. Wilson and D. K. Bruschek, "Machining of Selected Cast Aluminum Alloys with Compax Blank Tools," Paper presented at the International Conference on Cutting Tool Materials, SME, September 15 - 17, 1980.

[56] P. A. Bex, "Syndite For the Machining of Titanium Alloys," Industrial Diamond Review, August, 1977.

[57] "Diamond and Carbide Get it Together," Machinery and Production Engineering, May 2, 1979, pp. 26 - 27.

[58] P. A. Bex, "Syndite Cutting Tools - Preparation and Use," Syndite: Its Properties and Applications, A selection of papers presented at the DeBeers-Dusseldorf Conference, 1979, section 1.9.

[59] A. Milbrandt, "Space Vehicle Components Are Machined to High Precision By Diamond Turning," Industrial Diamond Review, April, 1976, pp. 134-138.

[60] B. M. Kramer and N. H. Cook, "Wear Resistant Coatings: The Group IVB and VB Carbides," NAMRC VIII, Rolla, MO, May 18-21, 1980.

[61] N. H. Cook, Manufacturing Analysis, Addison-Wesley, Reading, Massachusetts, 1966, p. 49.

[62] N. H. Cook and B. M. Kramer, "Tungsten Carbide Tools Treated with Group IVB and VB Metals," U.S. Patent Number 4,066,821, 1978.

[63] B. M. Kramer and N. P. Suh, "Tool Wear by Solution: A Quantitative Understanding," Trans. ASME, Journal of Engineering for Industry, Vol. 102, No. 3, November 1980, pp. 303-309.

[64] P. D. Hartung and B. M. Kramer, "Theoretical Considerations in the Machining of Nickel-Based Alloys," Proceedings of the International Conference on Cutting Tool Materials, ASM/SME/ISIJ/CIRP, Cincinnati, Ohio, September 15-17, 1980.

[65] E. Bickel, "The Temperature on a Turning Tool," International Research in Production Engineering, ASME, New York, 1963, pp. 89-94.

[66] W. G. Moffatt, The Handbook of Binary Phase Diagrams, General Electric Company, Schenectady, New York, 1981.

[67] E. Rudy, "Ternary Phase Equilibrion in Transition Metal-Boron-Carbon-Silicon Systems, Part V. Compendium of Phase Diagram Data," Technical Report AFML-TR-65-2, Part V, May 1969.

[68] M. Hansen, Constitution of the Binary Alloys, McGraw-Hill, New York, 1958.

[69] R. Elliott, Constitution of the Binary Alloys, First Supplement, McGraw-Hill, New York, 1965.

[70] N. Cook and P. Nayak, "The Thermal Mechanics of Tool Wear," Trans. ASME, Journal of Engineering for Industry, Vol. 88, No. 1, 1966, p. 93.

[71] R. C. Weast, ed., CRC Handbook of Chemistry and Physics, 60th Edition, CRC Press, Florida, 1980.

[72] R. J. Wasilewski and G. L. Kehl, "Diffusion of Nitrogen and Oxygen In Titanium," Journal of the Institute of Metals, Vol. 83, 1954-55, pp. 94-104.

[73] B. M. Kramer, Ph.D. Thesis, Department of Mechanical Engineering, M.I.T., 1979.

[74] W. B. Pearson, A Handbook of Lattice Spacings and Structures of Metals and Alloys, Volume 2, Pergamon Press, New York, 1967, p. 420.

[75] S. Ramalingam and J. D. Watson, "Tool Life Distributions, Part 4: Minor Phases in Work Materials and Multiple-Injury Tool Failure," Trans. ASME, Journal of Engineering for Industry, Vol. 100, May 1978, pp. 201-209.

[76] R. C. D. Richardson, "The Wear of Metals by Relatively Soft Abrasives," Wear, Vol. II, 1968, pp. 245-275.

[77] J. Larsen-Basse and P. A. Tanouye, "Abrasion of WC-Co Alloys by Loose Hard Abrasives," Advances in Hard Material Tool Technology, Proc. of the 1976 International Conference on Hard Material Tool Technology, Carnegie-Mellon University, Pittsburg, Pennsylvania, June 22-24, 1976, pp. 188-199.

[78] L. E. Davis et al., Handbook of Auger Electron Spectroscope, Second Edition, Physical Electronics Industries, Inc., Eden Prairie, Minnesota, 1976.

[79] A. D. McQuillan and M. K. McQuillan, Titanium, Butterworths Scientific Publications, London, 1956, p. 70.

[80] L. M. Adelsberg and L. H. Cadoff, "The Reactions of Liquid Titanium and Hafnium with Carbon," Transactions of the Metallurgical Society of AIME, Volume 239, June 1967, pp. 933-935.

[81] R. Hultgren et al., Selected Values of the Thermodynamic Properties of Binary Alloys, American Society for Metals, Metals Park, Ohio, 1973.

[82] J. Elliott, M. Gleiser and V. Ramakrishna, Thermochemistry for Steelmaking, Addison-Wesley, Reading, Massachusetts, 1963.

[83] H. Schick, Thermodyanmics of Certain Refractory Compounds, Academic Press, New York, 1966.

[84] D. Stull and H. Prophet, JANAF Thermochemical Tables, Second Edition, U.S. Superintendent of Documents Number C13.48:37, 1971.

[85] T. B. Reed, Free Energy of Formation of Binary Compounds: An Atlas of Charts for High-Temperature Chemical Calculations, M.I.T. Press, 1971.

[86] T. J. Yurick and K. E. Spear, "Thermodynamics of TiB_2 From Ti-B-N Studies," International Symposium on Thermodynamics of Nuclear Materials, IAEA-SM-236, Julich, Federal Republic of Germany, 1979, pp. 53-59.

[87] A. R. Miedema, F. R. de Boer and R. Boom, "Model Predictions For the Enthalpy of Formation of Transition Metal Alloys," CALPHAD, Vol. 1, No. 4, Pergamon Press, 1977, pp. 341-359.

[88] O. Kubaschewski and C. B. Alcock, Metallurgical Thermochemistry, Pergamon Press, New York, 1979, pp. 42-43.

[89] A. H. P. Skelland, Diffusional Mass Transfer, Wiley-Interscience, New York, 1974, pp. 110-117.

[90] Diffusion Data, Vol. 2, No. 3, Diffusion Information Center, Cleveland, Ohio, December 1968, p. 369.